

Complexes of Rhenium and Osmium with *o*-Phenylenediamine and *o*-Aminobenzenethiol. X-Ray Crystal Structures of $[Re\{o-(HN)_2C_6H_4\}_3][ReO_4]$, $Re[o-(HN)_2C_6H_4]_3$, $Re[o-(HN)_2C_6H_4]_2[o-(HN)NC_6H_4]$, $K[Re\{o-(HN)_2C_6H_4\}\{o-(HN)NC_6H_4\}_2]$, and $M[o-(HN)SC_6H_4]_3$ ($M = Re$ or Os)[†]

Andreas A. Danopoulos, Anthony C. C. Wong, and Geoffrey Wilkinson *

Johnson Matthey Laboratory, Chemistry Department, Imperial College, London SW7 2AY

Michael B. Hursthouse * and Bilquis Hussain

Chemistry Department, Queen Mary College, London E1 4NS

The interaction of trimethylsilyl perrhenate, $ReO_3(OSiMe_3)$, or Re_2O_7 , with *o*-phenylenediamine gives the homoleptic amido complex cation of rhenium(vii), $[Re\{o-(HN)_2C_6H_4\}_3]^+$, as its perrhenate salt. The cation can be reduced by sodium to the neutral rhenium(vi) species $Re[o-(HN)_2C_6H_4]_3$, which can be reoxidised by $AgPF_6$ to the cation as its hexafluorophosphate salt. Interaction of $[Re\{o-(HN)_2C_6H_4\}_3]^+$ with KOH leads to the singly and doubly deprotonated species, $Re[o-(HN)_2C_6H_4]_2[o-(HN)NC_6H_4]$ and $K[Re\{o-(HN)_2C_6H_4\}\{o-(HN)NC_6H_4\}_2]$. An improved preparation of the known amido thiolate $Re[(HN)SC_6H_4]_3$, i.e. interaction of $(H_2N)(HS)C_6H_4$ with $ReO_3^-(OSiMe_3)$, is described; the osmium analogue, $Os[(HN)SC_6H_4]_3$, is synthesised by interaction of the aminothiol with OsO_4 . Interaction of OsO_4 with $(H_2N)_2C_6H_4$ gives the complex *trans*- $OsO_2[(HN)C_6H_4]_2$. Infrared, 1H n.m.r., e.s.r., and electronic absorption and cyclic voltammetric data are given. The X-ray crystal structure of the cation $[Re\{o-(HN)_2C_6H_4\}_3]^+$ as the acetone solvate of the perrhenate shows a trigonal prismatic geometry, which is also confirmed for $Re[o-(HN)_2C_6H_4]_3$, $Re[o-(HN)_2C_6H_4]_2[o-(HN)NC_6H_4]$, $K[Re\{o-(HN)_2C_6H_4\}\{o-(HN)NC_6H_4\}_2]$, and $Re[(HN)SC_6H_4]_3$. The structure of $Os[o-(HN)SC_6H_4]_3$ shows it to have a slightly distorted octahedral geometry.

Transition-metal complexes of 1,2-dithiolenes and complexes derived from other unsaturated, chelating ligands, such as 1,2-dihydroxyarenes, 1,2-diaminoarenes, aminoarene thiols, etc. have been intensively studied because the complexes may be in apparently different oxidation states with reversible oxidation-reduction sequences as well as having unusual structural and chemical properties.¹ Examples of such complexes are $M[o-(HN)_2C_6H_4]_2$, $M = Ni$, Pd , Pt , or Co ,² $M[o-(HN)SC_6H_4]_3$, $M = Mo$,^{3a,b} Tc ,^{3b} or $Re^{3a,b}$ and $M(S_2C_2Ph_2)_3$, $M = Mo$, W , or Re .⁴

In this paper we describe compounds of rhenium and osmium derived from 1,2-diaminobenzene (*o*-phenylenediamine) and *o*-aminobenzenethiol.

For *o*-phenylenediamine the ligand can be in the reduced, dianionic, diamide form, $[o-(HN)_2C_6H_4]^{2-}$, the monoanionic, semibenzoquinone di-imide form, or the oxidised, neutral, benzoquinone di-imide form. The second and third forms have been isolated in, respectively, $M^{II}[o-(HN)_2C_6H_4]_2$, $M = Co$, Ni , Pd , or Pt ,² and $[Fe^{II}(CN)_4\{o-(HN)_2C_6H_4\}]^{2-}$,⁵ but the dianionic form, $[o-(HN)_2C_6H_4]^{2-}$, has not been isolated until the present work.

Although tris complexes of several types of these 'non-innocent,' unsaturated, chelating ligands are well known,¹ the only example⁶ of a tris species derived from *o*-phenylenediamine to be structurally characterised is a bis(1,2-benzoquinone di-imide)(1,2-benzosemiquinone di-imido) cobalt(II) ion which was obtained by air oxidation of the $[Co^{II}\{(o-H_2N)_2C_6H_4\}_3]^{2+}$ ion; it has a square pyramidal structure with the semiquinone ligand bound by only one nitrogen atom.

We have now synthesised the cation $[Re\{o-(HN)_2C_6H_4\}_3]^+$, whose structure has been confirmed as trigonal prismatic, like

many of the other tris species in high oxidation states. The reduction and deprotonation reactions have led to isolable complexes and in addition spectroscopic and electrochemical studies have been made.

An improved synthesis of the known^{3b} tris species $Re[o-(HN)SC_6H_4]_3$, is described, and the structure confirmed by X-ray diffraction study as being distorted trigonal prismatic: the technetium analogue and the isomorphous molybdenum complex have trigonal prismatic structures.^{3b} Other well characterised rhenium(vi) species are $Re(S_2C_2Ph_2)_3$,^{7a} $Re(1,2-S_2C_6H_3Me-4)_3$,^{7b} and catecholates.⁸

Similar studies on osmium have led to the complexes *trans*- $OsO_2[o-(HN)_2C_6H_4]_2$ and $Os[o-(HN)SC_6H_4]_3$; osmium species of similar type are tris(catecholates),⁹ $Os(S_2C_2Ph_2)_3$,¹⁰ and $Os(1,2-S_2C_6H_3Me-4)_3$.¹¹

Analytical data for the new compounds are given in Table 1, 1H n.m.r. data in Table 2.

Results and Discussion

Rhenium Compounds.—The tris(*o*-phenylenediamido)rhenium(vii) ion. The interaction of trimethylsilyl perrhenate, $ReO_3(OSiMe_3)$, Re_2O_7 , or, less effectively, $NBu_4^nReO_4$ with an excess of *o*-phenylenediamine in tetrahydrofuran (thf) gives a deep green solution, from which the salt, $[Re(o-pda)_3][ReO_4]$ (I) [$\text{o-pda} = o-(HN)_2C_6H_4^{2-}$], can be isolated as air-stable, deep green/red dichroic prisms. The solubility in most polar solvents is low but the salt can be crystallised from acetone as a 1:1 solvate. The conductivity in MeCN is that for a 1:1 electrolyte. The X-ray crystal structure of the compound is discussed later. The i.r. spectrum has bands at 3 296 [v(N-H)], 1 551 [v(C=C)], 908, 899, 890 [v(Re=O)], and 573 cm^{-1} [v(Re-N)]. When crystallised from acetone the spectrum has an additional band at 1 695 cm^{-1} [v(C=O)].

† Supplementary data available: see Instructions for Authors, *J. Chem. Soc., Dalton Trans.*, 1990, Issue 1, pp. xix–xxii.

Table 1. Analytical data for complexes of rhenium and osmium

Compound	Colour	M.p. (°C)	Analysis (%) ^a			
			C	H	N	Other
[Re(<i>o</i> -pda) ₃][ReO ₄]·Me ₂ CO	Green/red ^b	>340	30.4 (31.0)	2.9 (2.9)	10.5 (10.3)	9.1 (O) (9.82)
[Re(<i>o</i> -pda) ₃]PF ₆	Green/red ^b	>320	33.7 (33.3)	3.0 (2.8)	12.5 (12.9)	5.0 (P) (4.8)
Re(<i>o</i> -pda) ₃	Red-violet	>300	42.9 (42.7)	3.6 (3.8)	16.7 (16.5)	
Re(<i>o</i> -pda) ₂ (<i>o</i> -pbqd)·CH ₂ Cl ₂	Red	125—127	39.2 (38.8)	2.8 (3.2)	13.9 (14.3)	
K[Re(<i>o</i> -pda)(<i>o</i> -pbqd) ₂]	Red-brown	ca. 300	39.8 (39.9)	2.9 (3.0)	14.8 (15.5)	
Re(abt) ₃	Blue/purple ^b	>310	39.3 (38.9)	2.7 (2.7)	7.5 (7.6)	16.9 (S) (17.3)
Os(abt) ₃ ·CH ₂ Cl ₂	Red	98—100	34.9 (35.4)	2.4 (2.6)	6.6 (6.5)	15.2 (S) (14.9)
OsO ₂ (<i>o</i> -pda) ₂	Brown	>320	34.4 (33.2)	2.8 (2.8)	12.6 (12.9)	

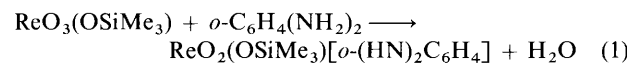
^a Calculated values in parentheses. ^b Dichroic crystals.

The ¹H n.m.r. spectrum has a broad singlet at δ 13.64(1), assignable to NH and a well resolved AA'BB' (tending to AA'XX') pattern of two sets of sextets at δ 7.44(1) and 7.03(1) [J_{AA'} = 0.03, J_{AB} = 8.25, J_{BB'} = 6.36, and J_{AB'} = 1.10 Hz] due to the aromatic ring protons. However, these shifts alone are not diagnostic with regard to the various possible oxidation states of the ligand, but since there is only one set of splitting pattern the ligands are evidently identical on the n.m.r. time-scale. Furthermore, the ¹H-¹H coupling constants do suggest aromaticity of the ring, consistent with the diamido form of the ligand and are similar to those of benzotriazole (Table 3) in contrast to 2-methylbenzotriazole, which is analogous to the di-imido system and shows loss of aromaticity (low J_{AB'}) and strong and weak bonding between A-B and B-B' positions respectively.

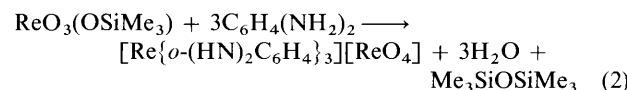
The complex is weakly paramagnetic in the solid state ($\mu_{\text{eff.}} = 0.6$ per Re) evidently due to the temperature-independent paramagnetism as found in other rhenium(vii) compounds.^{3a,12} The semibenzoquinone di-imide ligand form would require a rhenium(IV), paramagnetic species.

The above evidence for the diamido ligand form is confirmed by the structural and electrochemical studies discussed later.

The very rapid reaction between *o*-C₆H₄(NH₂)₂ and ReO₃(OSiMe₃) presumably involves an initial condensation as in equation (1). Hydrolysis of the siloxide will remove water as



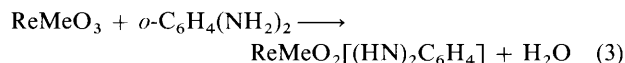
Me₃SiOH, H⁺, and ReO₄⁻. Further condensations will occur with ReO₄⁻ and the reaction may in part be driven by the low solubility of the product. Addition of molecular sieves to remove water makes no obvious difference either to the rate or to the yield of product. The overall stoichiometry appears to be as in equation (2) and the reaction is essentially quantitative based on



ReC₆H₄(OSiMe₃). A similar mechanism doubtless applies for Re₂O₇. The cation can be obtained as its PF₆⁻ salt as noted below.

Evidence for reaction (1) is provided by that between

ReMeO₃ and *o*-phenylenediamine which leads to the trigonal bipyramidal amido molecule as in equation (3). This work will



be described separately. A similar reaction occurs with OsO₄ (see later).

*Reduction of [Re(*o*-pda)₃][ReO₄]; Re(*o*-pda)₃.* The reaction of [Re(*o*-pda)₃][ReO₄] with excess of sodium in thf gave the paramagnetic compound, Re(*o*-pda)₃ (**2**), as a red-violet, crystalline solid, giving deep violet solutions in most organic solvents. The other product in the reaction is an insoluble, pale cream solid, presumably from reduction of perrhenate. The i.r. spectrum of (**2**) is similar to that of [Re(*o*-pda)₃]⁺ with ν(N-H) at 3 293 cm⁻¹, ν(C=C) at 1 563 cm⁻¹, and ν(Re-N) at 573 cm⁻¹; the Re-O stretch is not, of course, present. The e.s.r. spectrum of (**2**) is discussed later.

The ¹H n.m.r. spectrum consists of broad, poorly resolved peaks due to the paramagnetism; the amido proton signal is not observed. An AA'BB' splitting pattern for the aromatic protons, consisting of two sets of sextets centred at ca. δ 6.63 and 6.48, is just discernible.

The oxidation of the neutral species to the cation can be made cleanly with AgPF₆ in thf and [Re(*o*-pda)₃]PF₆ isolated as air-stable prisms; the solubility of this hexafluorophosphate is higher than that of the perrhenate in polar solvents. The i.r. and n.m.r. spectra are similar for both salts.

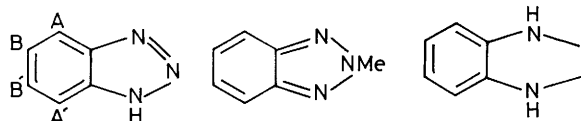
*Reactions of [Re(*o*-pda)₃]⁺ with base.* The interaction of [Re(*o*-pda)₃][ReO₄] in acetone with a small excess of methanolic KOH resulted in a good yield (ca. 74%) of the neutral, singly deprotonated product, formulated as Re[*o*-(HN)₂C₆H₄]₂[*o*-(HN)NC₆H₄] (**3**), with two phenylenediamide and one pseudo-benzoquinone di-imide (pbqd) ligands.

The red, crystalline compound gives deep red solutions in most polar organic solvents, and is diamagnetic and a non-electrolyte in MeCN. The i.r. spectrum has a strong, fairly broad band at 3 264 cm⁻¹, and a sharp band at 1 561 cm⁻¹, which were assigned, by comparison with [Re(*o*-pda)₃]⁺, to ν(N-H) and ν(C=C) respectively. In the ν(Re-N) region there are now at least two bands at 583 and 568 cm⁻¹. This may be due to the asymmetry in the nitrogen environments. There is also a band at 1 594 cm⁻¹ assigned tentatively to ν(C=N). Crystallisation from acetone gives an adduct with ν(C=O) at 1 702 cm⁻¹.

Table 2. Proton n.m.r. spectra of rhenium and osmium compounds^a

Compound	δ	Assignment
[Re(<i>o</i> -pda) ₃][ReO ₄]	13.64 (br, 1)	<i>o</i> -C ₆ H ₄ (NH) ₂
	7.44 (sxt, 1) ^b	<i>o</i> -C ₆ H ₄ (NH) ₂ (H _A , H _{A'})
	7.03 (sxt, 1) ^b	<i>o</i> -C ₆ H ₄ (NH) ₂ (H _B , H _{B'})
[Re(<i>o</i> -pda) ₃]PF ₆ ^c	13.54 (br, 1)	<i>o</i> -C ₆ H ₄ (NH) ₂
	7.446 (sxt, 1) ^d	<i>o</i> -C ₆ H ₄ (NH) ₂ (H _A , H _{A'})
	7.038 (sxt, 1) ^e	<i>o</i> -C ₆ H ₄ (NH) ₂ (H _B , H _{B'})
Re(<i>o</i> -pda) ₃	6.63 (sxt, 1) ^f	<i>o</i> -C ₆ H ₄ (NH) ₂ (H _A , H _{A'})
	6.48 (sxt, 1) ^f	<i>o</i> -C ₆ H ₄ (NH) ₂ (H _B , H _{B'})
Re(abt) ₃	7.45 (dd, 1) ^g	<i>o</i> -C ₆ H ₄ (NH)S (H _A)
	6.98 (dd, 1) ^h	<i>o</i> -C ₆ H ₄ (NH)S (H _D)
	6.78 (m, 1) ⁱ	<i>o</i> -C ₆ H ₄ (NH)S (H _B)
	6.53 (m, 1) ⁱ	<i>o</i> -C ₆ H ₄ (NH)S (H _C)
Re(<i>o</i> -pda) ₂ (<i>o</i> -pbqd)	11.43 (br)	NH
	8.55 (dd, 1) ^j	<i>o</i> -C ₆ H ₄ (NH) ₂ (H _A)
	8.44 (dd, 1) ^j	<i>o</i> -C ₆ H ₄ (NH) ₂ (H _D)
	7.918 (m, 1) ^k	<i>o</i> -C ₆ H ₄ (NH) ₂ (H _B)
	7.743 (m, 1) ^k	<i>o</i> -C ₆ H ₄ (NH) ₂ (H _C)
	8.045 (dd, 1) ^j	<i>o</i> -C ₆ H ₄ (NH) ₂ (H _A)
	7.670 (dd, 1) ^j	<i>o</i> -C ₆ H ₄ (NH) ₂ (H _D)
	7.315 (m, 1) ^l	<i>o</i> -C ₆ H ₄ (NH) ₂ (H _C)
	6.10 (2dd, 2) ^m	<i>o</i> -C ₆ H ₄ (NH) ₂ (H _A , H _D)
	6.155 (m, 1)	<i>o</i> -C ₆ H ₄ (NH) ₂ (H _B)
	5.98 (m, 1) ⁿ	<i>o</i> -C ₆ H ₄ (NH) ₂ (H _C)
Os(abt) ₃	12.22 (br, 1)	<i>o</i> -C ₆ H ₄ (NH)S
	7.59 (dd, 1) ^o	<i>o</i> -C ₆ H ₄ (NH)S (H _A)
	7.57 (dd, 1) ^o	<i>o</i> -C ₆ H ₄ (NH)S (H _D)
	7.02 (m, 1) ^p	<i>o</i> -C ₆ H ₄ (NH)S (H _B)
	6.86 (m, 1) ^p	<i>o</i> -C ₆ H ₄ (NH)S (H _C)
OsO ₂ (<i>o</i> -pda) ₂	10.42 (br, 1)	<i>o</i> -C ₆ H ₄ (NH) ₂
	6.94 (sxt, 1) ^p	<i>o</i> -C ₆ H ₄ (NH) ₂ (H _A , H _{A'})
	6.56 (sxt, 1) ^p	<i>o</i> -C ₆ H ₄ (NH) ₂ (H _A , H _B)

^a sxt = sextet, dd = doublet of doublets, and spt = septet. ^b $J_{AA'} = 0.03$, $J_{AB} = 8.25$, $J_{BB'} = 6.36$, and $J_{AB'} = 1.10$ Hz. ^c $^{31}\text{P} = -139.6$ (spt), $J_{\text{P}-\text{F}} = 711$ Hz. ^d Separation of outer lines 15.5 Hz. ^e Separation of outer lines 16.5 Hz. ^f Broad and poorly defined. ^g $J_{AB} = 7.7$ Hz. ^h $J_{CD} = 7.7$ Hz. ⁱ Multiplet comprises of a triplet in between two doublets. Separation of outer lines ca. 15 Hz. ^j J_{AB} , $J_{CD} = 8.75$ Hz. ^k Multiplet comprises of a triplet between two doublets. Separation of outer lines ca. 16.88 Hz. ^l Separation of outer lines ca. 17.5 Hz. ^m Signal comprises of two coalesced sets of doublets of doublets. ⁿ Separation of outer lines ca. 16.25 Hz. ^o J_{AB} , $J_{CD} \approx 5$ Hz. ^p Separation of outer lines ca. 17 Hz.

Table 3. Proton-proton coupling constants (Hz) in the *o*-phenylenediamido ligand of [Re(pda)₃][ReO₄]^aBenzotriazole 2-Methylbenzotriazole *o*-Phenylenediamido

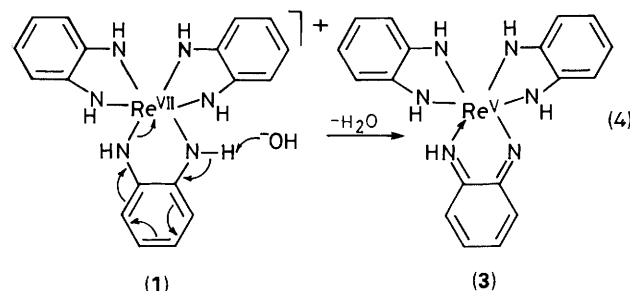
Compound	J_{AB}	$J_{BB'}$	$J_{AB'}$
Benzotriazole*	8.3	6.7	1.4
<i>o</i> -Phenylenediamido	8.25	6.36	1.10
2-Methylbenzotriazole*	9.4	3.6	0.5

* See 'Comprehensive Heterocyclic Chemistry,' eds. A. R. Katritzky and C. W. Rees, Pergamon, Oxford, 1984, vol. 5, sect. 15.

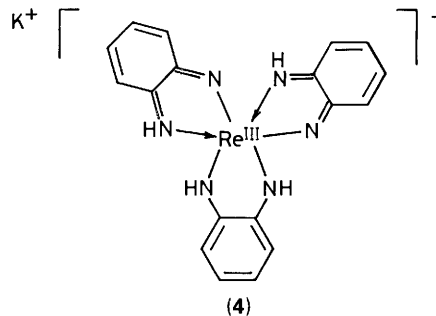
The ^1H n.m.r. spectrum has a broad singlet at δ 11.43, assigned to the NH protons, and a complex series of peaks between δ 5.9 and 8.6 from the ring protons (see Figure 1). The series consists of three sets (labelled a, b, and c) of ABCD splitting patterns, each set comprising a pair of doublets of doublets (H_A , H_D) and a pair of multiplets (H_B , H_C ; each made

up of a triplet in between two doublets) (see Table 2). The second multiplet from set b is hidden under the peaks at δ 7.6–7.8, as indicated by the integration. Part of one multiplet of set c is at the low-field edge of the peaks at δ 6.05–6.2. The rest of the peaks in this region are derived from the coalescence of the pair of doublets of doublets. This again agrees well with the integration. The low-field peaks of the spectrum (δ 7.25–8.6, sets a and b) result from the phenylenediamido ligands and are consistent with the aromaticity in the rings. The high-field peaks (δ 5.9–6.2, set c) result from the pseudo-benzoquinone di-imido ligand, and are consistent with the conjugated double-bond structure of the ring. The nitrogens in the *o*-phenylenediamido ligands are no longer equivalent due to the presence of the pseudo-benzoquinone di-imido ligand.

Complex (3) is hence formulated as one of Re^V as in equation (4).



Interaction of Re(*o*-pda)₂(*o*-pbqd) with a large excess of KOH in acetone gave a high yield (ca. 81%) of the brown-red, doubly deprotonated product, (4). This compound gives brown



solutions in polar organic solvents and is a 1:1 electrolyte in MeCN. The i.r. spectrum of (4) is very similar to that of the singly deprotonated compound (3), with bands at 1601 and 1560 cm⁻¹, assigned to v(C=N) and v(C=C). There are also bands at 561 and 585 cm⁻¹, which may again be due to v(Re-N).

The rhenium centre is now formally in the III oxidation state. The compound is paramagnetic, but the solid-state magnetic moment (1.6) (which is low for two unpaired electrons due to spin-orbit coupling) agrees well with those for mononuclear octahedral rhenium(III) complexes ($\mu_B = 1.5$ –2.1).¹³ The ^1H n.m.r. spectrum showed broad, poorly resolved peaks in the same general area as that of the singly deprotonated compound (Table 2). The low-field peaks for the *o*-phenylenediamido ring protons are at ca. δ 7.0–8.5 and the high-field peaks for the imido aromatic ring protons are at ca. δ 5.2–6.2. The amido proton signal is not observed [*cf.* Re(abt)₃ below].

Re(abt)₃. The complex Re(abt)₃ [abt = *o*-(HN)SC₆H₄²⁻] was previously^{3a} prepared by reaction of *o*-aminobenzenethiol with KReO₄ in acidic aqueous ethanol to give, initially, a compound tentatively formulated as Re(C₆H₄NS)(C₆H₄NHS)₂ which was then treated with acetone over several days to give a moderate yield of Re(abt)₃, (5).

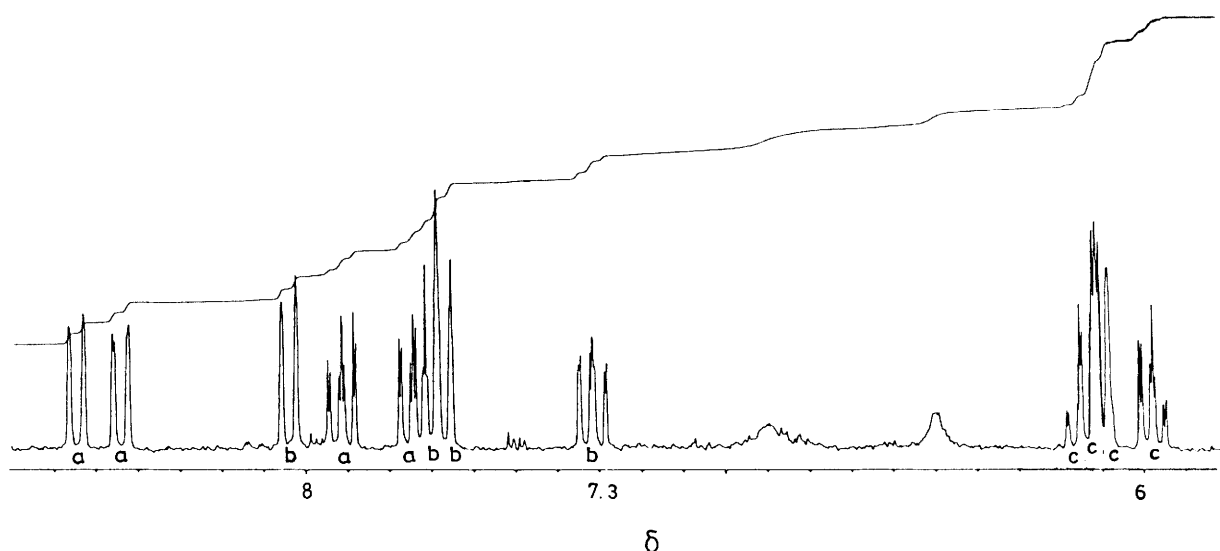


Figure 1. The ^1H n.m.r. spectrum of $\text{Re}(\text{o-pda})_2(\text{o-pbqd})$

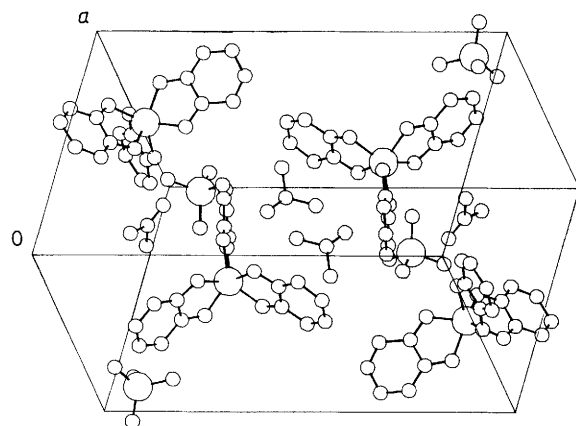


Figure 2. Unit cell of $[\text{Re}(\text{o-pda})_3][\text{ReO}_4]\cdot\text{Me}_2\text{CO}$

Reaction of the aminothiol in slight excess with $\text{ReO}_3\cdot(\text{OSiMe}_3)$ in thf in the presence of molecular sieves rapidly gives the complex in good yield as air-stable deep blue/purple dichroic prisms. The properties agree with those reported.^{3a,b} The i.r. spectrum has bands at 3 225(vN–H), 1 547(vC=C), and at 571 cm⁻¹, the latter being assigned as v(Re–N) by comparison with the spectrum of $[\text{Re}(\text{o-pda})_3]^+$; a band at 323 cm⁻¹ may be assigned to v(Re–S) (*c.f.* ref. 14). Although paramagnetic, the ^1H n.m.r. spectrum is sharp with an ABCD splitting pattern of two doublets of doublets at δ 7.45(1) and 6.98(1) (H_A , H_D ; $J_{\text{AB}} = J_{\text{CD}} = 7.7$ Hz) and two multiplets, each comprising a triplet between two doublets, at δ 6.78(1) and 6.53(1) (H_B , H_C ; separation of outer line *ca.* 15 Hz), assigned to the aromatic protons. The NH resonance is not observed, presumably due to the broadening by the nitrogen quadrupole¹⁵ exacerbated by the unpaired electron spin.

The formation of a rhenium(vi) complex from aminobenzenethiol rather than a rhenium(vii) cation as with *o*-phenylenediamine is probably due to the more reducing nature of the aminothiol.

X-Ray crystal structures of $[\text{Re}(\text{o-pda})_3][\text{ReO}_4]$, $\text{Re}(\text{o-pda})_3$, $\text{Re}(\text{o-pda})_2(\text{o-pbqd})$, $\text{K}[\text{Re}(\text{o-pda})(\text{o-pbqd})_2]$ and $\text{Re}(\text{abt})_3$. The perrhenate salt (**1**) crystallizes as an acetone solvate with two crystallographically independent formula units, $[\text{Re}(\text{o-pda})_3]\cdot[\text{ReO}_4]\cdot\text{Me}_2\text{CO}$, in the asymmetric unit (Figure 2). The co-ordination geometries around the two cationic metal centres are

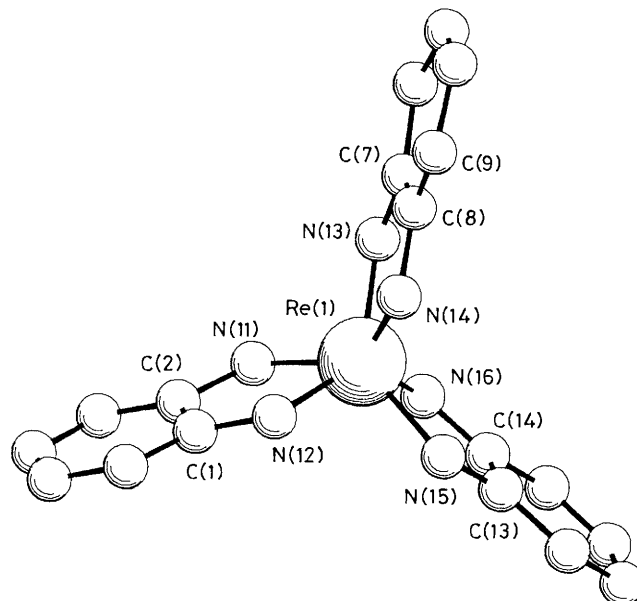


Figure 3. View of the cation $[\text{Re}(\text{o-pda})_3]^+$

almost perfect trigonal prismatic. Geometry parameters are given in Table 4 and diagrams of one of the two independent cations in Figures 3 and 4.

The occurrence of, and bonding in, trigonal prismatic $\text{M}(\text{XX}')_3$ species has been much discussed in the literature and various factors have been suggested to account for the stability of this geometry or deviations from it.^{4,16-21} Features of the geometry of those structures that are very close to the ideal trigonal prism are the prism dimensions, expressed in terms of the ratio of the side of the trigonal face and the prism height, s/h ,¹⁹ which is directly related to the relative inter- and intra-ligand $\text{X}\cdots\text{X}'$ distances, the actual $\text{M}-\text{X},\text{X}'$ distances which may be used to discuss the nature of the $\text{M}-\text{X},\text{X}'$ bonding, especially the presence or not of π interactions,²¹ and folding of the ligands about the $\text{X}\cdots\text{X}'$ line which is discussed in terms of $\text{M}-\text{X},\text{X}'$, π bonding, $\text{X}\cdots\text{X}$ interligand bonding, or packing effects.¹⁹

It is not necessary to reiterate here these discussions but only to report that in this $[\text{Re}(\text{o-pda})_3]^+$, ReN_6 , species, as in

Table 4. Bond lengths (\AA) and angles ($^\circ$) for compound (**1**)

N(11)–Re(1)	1.974(21)	N(12)–Re(1)	2.023(23)	C(12B)–N(23)	1.271(33)	C(7B)–N(24)	1.286(38)
N(13)–Re(1)	1.996(24)	N(14)–Re(1)	1.981(21)	C(14B)–N(25)	1.325(36)	C(13B)–N(26)	1.378(44)
N(15)–Re(1)	1.994(26)	N(16)–Re(1)	2.016(22)	C(2B)–C(1B)	1.485(37)	C(6B)–C(1B)	1.479(43)
C(2A)–N(11)	1.392(32)	C(1A)–N(12)	1.324(31)	C(2B)–C(3B)	1.378(39)	C(3B)–C(4B)	1.371(45)
C(7A)–N(13)	1.329(27)	C(8A)–N(14)	1.377(35)	C(4B)–C(5B)	1.422(48)	C(5B)–C(6B)	1.313(46)
C(13A)–N(15)	1.336(35)	C(14A)–N(16)	1.328(41)	C(8B)–C(7B)	1.524(38)	C(12B)–C(7B)	1.422(38)
C(2A)–C(1A)	1.425(36)	C(3A)–C(1A)	1.420(39)	C(9B)–C(8B)	1.328(55)	C(10B)–C(9B)	1.438(48)
C(4A)–C(3A)	1.335(41)	C(5A)–C(4A)	1.437(46)	C(11B)–C(10B)	1.381(39)	C(12B)–C(11B)	1.367(46)
C(6A)–C(5A)	1.398(43)	C(6A)–C(2A)	1.401(35)	C(14B)–C(13B)	1.416(47)	C(18B)–C(13B)	1.385(43)
C(8A)–C(7A)	1.449(37)	C(12A)–C(7A)	1.437(38)	C(15B)–C(14B)	1.450(53)	C(16B)–C(15B)	1.371(49)
C(9A)–C(8A)	1.358(30)	C(10A)–C(9A)	1.405(42)	C(17B)–C(16B)	1.369(56)	C(18B)–C(17B)	1.454(54)
C(11A)–C(10A)	1.449(45)	C(12A)–C(11A)	1.341(35)	O(10)–Re(3)	1.693(23)	O(20)–Re(3)	1.709(22)
C(14A)–C(13A)	1.442(44)	C(18A)–C(13A)	1.379(44)	O(30)–Re(3)	1.702(25)	O(40)–Re(3)	1.743(23)
C(15A)–C(14A)	1.522(47)	C(16A)–C(15A)	1.329(54)	O(50)–Re(4)	1.706(18)	O(60)–Re(4)	1.677(26)
C(17A)–C(16A)	1.375(51)	C(18A)–C(17A)	1.400(44)	O(70)–Re(4)	1.725(20)	O(80)–Re(4)	1.737(22)
N(21)–Re(2)	1.989(23)	N(22)–Re(2)	1.995(25)	C(20A)–C(10A)	1.481(69)	C(30A)–C(10A)	1.472(74)
N(23)–Re(2)	2.010(26)	N(24)–Re(2)	2.025(20)	O(10A)–C(10A)	1.198(48)	C(20B)–C(10B)	1.430(44)
N(25)–Re(2)	2.005(29)	N(26)–Re(2)	2.038(24)	C(30B)–C(10B)	1.554(46)	O(10B)–C(10B)	1.208(37)
C(2B)–N(21)	1.336(37)	C(1B)–N(22)	1.283(36)				
N(12)–Re(1)–N(11)	77.4(9)	N(13)–Re(1)–N(11)	86.5(9)	N(25)–Re(2)–N(24)	87.3(10)	N(26)–Re(2)–N(21)	84.4(10)
N(13)–Re(1)–N(12)	132.4(8)	N(14)–Re(1)–N(11)	133.9(9)	N(26)–Re(2)–N(22)	133.0(10)	N(26)–Re(2)–N(23)	86.0(11)
N(14)–Re(1)–N(12)	83.0(10)	N(14)–Re(1)–N(13)	76.8(10)	N(26)–Re(2)–N(24)	134.9(10)	N(26)–Re(2)–N(25)	77.3(11)
N(15)–Re(1)–N(11)	132.0(8)	N(15)–Re(1)–N(12)	85.6(10)	C(2B)–N(21)–Re(2)	122.1(18)	C(2B)–C(1B)–N(22)	113.6(25)
N(15)–Re(1)–N(13)	134.6(9)	N(15)–Re(1)–N(14)	86.6(10)	C(6B)–C(1B)–N(22)	130.5(26)	C(6B)–C(1B)–C(2B)	115.0(24)
N(16)–Re(1)–N(15)	76.6(10)	N(16)–Re(1)–N(11)	85.7(9)	C(1B)–C(2B)–N(21)	108.2(23)	C(3B)–C(2B)–N(21)	131.1(24)
N(16)–Re(1)–N(12)	136.7(7)	N(16)–Re(1)–N(13)	85.0(9)	C(3B)–C(2B)–C(1B)	120.7(26)	C(4B)–C(3B)–C(2B)	119.5(27)
N(16)–Re(1)–N(14)	133.8(9)	C(2A)–N(11)–Re(1)	119.0(17)	C(5B)–C(4B)–C(3B)	122.3(30)	C(6B)–C(5B)–C(4B)	120.4(32)
C(1A)–N(12)–Re(1)	116.7(18)	C(7A)–N(13)–Re(1)	120.8(19)	C(5B)–C(6B)–C(1B)	121.5(30)	C(12B)–N(23)–Re(2)	124.1(20)
C(8A)–N(14)–Re(1)	118.0(19)	C(13A)–N(15)–Re(1)	119.6(20)	C(7B)–N(24)–Re(2)	116.7(17)	C(8B)–C(7B)–N(24)	124.8(25)
C(14A)–N(16)–Re(1)	117.2(19)	C(2A)–C(1A)–N(12)	116.3(22)	C(12B)–C(7B)–N(24)	118.1(22)	C(12B)–C(7B)–C(8B)	117.0(27)
C(3A)–C(1A)–N(12)	123.6(24)	C(3A)–C(1A)–C(2A)	119.9(23)	C(9B)–C(8B)–C(7B)	119.6(28)	C(10B)–C(9B)–C(8B)	119.6(29)
C(1A)–C(2A)–N(11)	110.4(21)	C(6A)–C(2A)–N(11)	126.9(24)	C(11B)–C(10B)–C(9B)	122.0(33)	C(12B)–C(11B)–C(10B)	120.0(29)
C(6A)–C(2A)–C(1A)	122.6(24)	C(4A)–C(3A)–C(1A)	117.9(27)	C(7B)–C(12B)–N(23)	107.4(27)	C(11B)–C(12B)–N(23)	131.3(25)
C(5A)–C(4A)–C(3A)	121.9(29)	C(6A)–C(5A)–C(4A)	122.3(27)	C(11B)–C(12B)–C(7B)	121.4(24)	C(14B)–N(25)–Re(2)	114.3(22)
C(5A)–C(6A)–C(2A)	114.9(25)	C(8A)–C(7A)–N(13)	111.1(23)	C(13B)–N(26)–Re(2)	118.7(21)	C(14B)–C(13B)–N(26)	107.6(26)
C(12A)–C(7A)–N(13)	130.0(25)	C(12A)–C(7A)–C(8A)	118.7(20)	C(18B)–C(13B)–N(26)	124.5(33)	C(18B)–C(13B)–C(14B)	127.6(34)
C(7A)–C(8A)–N(14)	113.2(19)	C(9A)–C(8A)–N(14)	126.8(25)	C(13B)–C(14B)–N(25)	121.1(31)	C(15B)–C(14B)–N(25)	124.4(30)
C(9A)–C(8A)–C(7A)	120.0(24)	C(10A)–C(9A)–C(8A)	120.3(26)	C(15B)–C(14B)–C(13B)	114.0(27)	C(16B)–C(15B)–C(14B)	120.0(35)
C(11A)–C(10A)–C(9A)	119.8(23)	C(12A)–C(11A)–C(10A)	119.9(28)	C(17B)–C(16B)–C(15B)	122.9(39)	C(18B)–C(17B)–C(16B)	120.6(31)
C(11A)–C(12A)–C(7A)	120.3(28)	C(14A)–C(13A)–N(15)	111.4(26)	C(17B)–C(18B)–C(13B)	114.0(32)	O(20)–Re(3)–O(10)	105.2(11)
C(18A)–C(13A)–N(15)	131.0(26)	C(18A)–C(13A)–C(14A)	117.6(26)	O(30)–Re(3)–O(10)	106.5(12)	O(30)–Re(3)–O(20)	114.0(12)
C(13A)–C(14A)–N(16)	114.8(26)	C(15A)–C(14A)–N(16)	126.9(30)	O(40)–Re(3)–O(10)	110.7(11)	O(40)–Re(3)–O(20)	109.7(11)
C(15A)–C(14A)–C(13A)	118.3(30)	C(16A)–C(15A)–C(14A)	116.1(32)	O(40)–Re(3)–O(30)	110.6(11)	C(30A)–C(10A)–C(20A)	116.4(42)
C(17A)–C(16A)–C(15A)	127.1(33)	C(18A)–C(17A)–C(16A)	116.4(33)	O(10A)–C(10A)–C(20A)	122.2(39)	O(10A)–C(10A)–C(30A)	119.3(40)
C(17A)–C(18A)–C(13A)	124.4(30)	N(22)–Re(2)–N(21)	74.9(10)	O(60)–Re(4)–O(50)	110.1(10)	O(70)–Re(4)–O(50)	108.7(10)
N(23)–Re(2)–N(21)	88.5(10)	N(23)–Re(2)–N(22)	133.8(9)	O(70)–Re(4)–O(60)	108.1(11)	O(80)–Re(4)–O(50)	108.8(10)
N(24)–Re(2)–N(21)	133.1(8)	N(24)–Re(2)–N(22)	87.0(9)	O(80)–Re(4)–O(60)	111.5(11)	O(80)–Re(4)–O(70)	109.7(11)
N(24)–Re(2)–N(23)	73.4(9)	N(25)–Re(2)–N(22)	86.7(11)	C(30B)–C(10B)–C(20B)	115.9(28)	O(10B)–C(10B)–C(20B)	123.8(26)
N(25)–Re(2)–N(21)	133.0(9)	N(25)–Re(2)–N(23)	132.0(10)	O(10B)–C(10B)–C(30B)	120.2(25)		

$\text{Re}(\text{S}_2\text{C}_2\text{Me}_2)_3$,⁷ there is no fold of the ligands, that the prism is compressed, with a value for s/h of 1.12, and that the Re–N distances are seemingly short, at an average of 2.00 Å.

The compression of the prism is related to the smaller bite of the N,N ligand compared with S,S ligands. Thus the average N–Re–N angle in $[\text{Re}(o\text{-pda})_3]^+$ is 76.9° compared with S–Re–S of 81.4° in $\text{Re}(\text{S}_2\text{C}_2\text{Ph}_2)_3$. It is also likely in the ReN_6 structure that the interligand N...N contacts, 2.71 Å, although less than the van der Waals diameter of 3.00 Å, are non-bonding.

As mentioned earlier, the Re–N distances are considered to be shorter than expected single-bond values; thus we may compare them with the values for the Re–N(amido) bond length of 2.20 Å in $\text{Re}(\text{NHPh})(\text{N}_2)(\text{PMe}_3)_4$ ²¹ where there is no π character associated with this bond. For the formally 12e ReN_6 system here, with filled π_v^4 (*i.e.* perpendicular to the ligand plane) orbitals on the nitrogens, N–M π bonding is to

be expected with three such interactions ‘shared’ between the six bonds.

The N–C bonds in the ligand, whose lengths average 1.35(3) Å, also seem to have multiple-bond character but with no statistically significant pattern of long/short bonds in the aromatic ring; indeed, all the evidence is for electron delocalisation over the whole molecule. This may be significant in stabilising the high oxidation states in these complexes.

The structure of the neutral reduced species $\text{Re}(o\text{-pda})_3 \cdot 2\text{C}_4\text{H}_8\text{O}$ (**2**) has been determined; a diagram of the molecule of $\text{Re}(o\text{-pda})_3$, together with the atomic numbering scheme, is given in Figure 5; bond lengths and angles are in Table 5. The co-ordination geometry is again that of an almost ideal trigonal prism, with no fold of the ligand. The metal–nitrogen bond distances are equal within experimental error at 2.00–2.01(1) Å and equal to those in the cation, described above. Similarly, the N–Re–N bite angles, 74.8–75.3(4)°, the prism parameter s/h ,

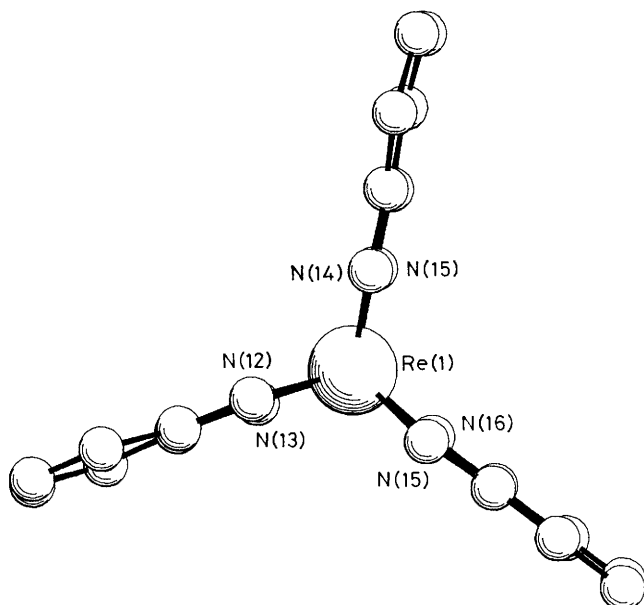


Figure 4. View of the cation in Figure 3 along the approximate C_3 axis

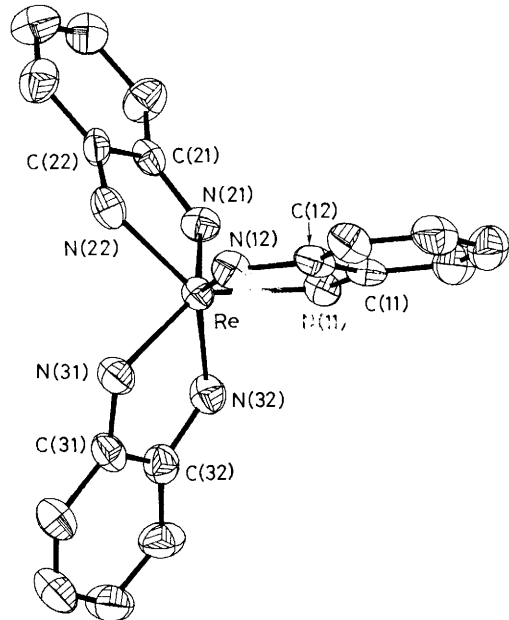


Figure 5. Molecular structure of $\text{Re}(\text{o-pda})_3$

1.13, and the $\text{N}\cdots\text{N}$ non-bonded prism contacts, 2.74—2.78 Å, are also very similar to values for the cation. This close similarity agrees with the suggestion^{3b} (see e.s.r. discussion later) that the unpaired electron sits mainly in ligand orbitals, so the electronic configuration at the metal in the formally rhenium-(vii) and -(vi) complexes can be considered to be equivalent. However, as a result of the lower precision to which light atoms can be located in these heavy-atom structures, the ligand geometries in the two complexes do not show any significant differences.

The neutral monodeprotonated compound $[\text{Re}(\text{o-pda})_2(\text{o-pbqd})]$ (3) crystallises isostructurally with $\text{Re}(\text{o-pda})_3$, as a tetrahydrofuran solvate. As might be expected, the site of deprotonation is not detectable and we presume that the molecule disorders so that all six N sites are equivalent. Indeed, the cell dimensions and co-ordinates, and thus geometry

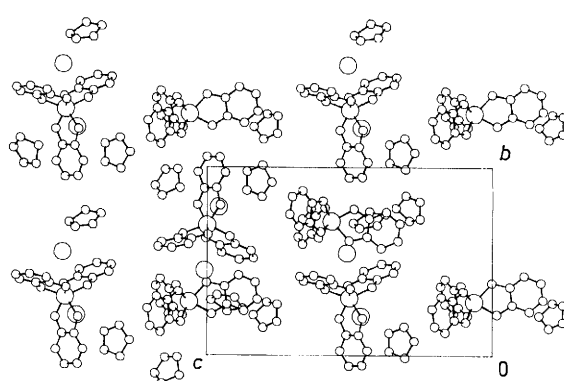


Figure 6. Packing of the components of the structure of $\text{K}[\text{Re}(\text{o-pda})(\text{o-pbqd})_2]\cdot\text{C}_4\text{H}_8\text{O}$. Only the lower half of the cell is shown, to reduce overlap

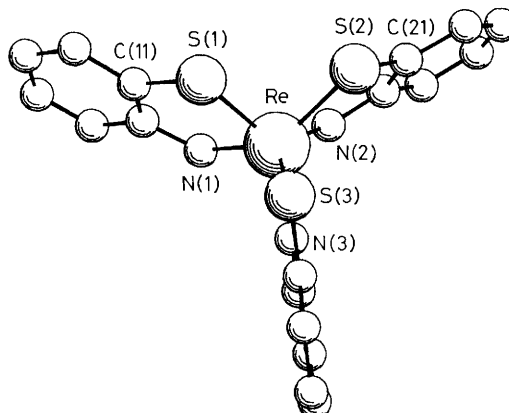


Figure 7. Molecular structure of $\text{Re}(\text{abt})_3$

parameters for $\text{Re}(\text{o-pda})(\text{o-pbqd})$, are indistinguishable from those of $\text{Re}(\text{o-pda})_3$. The individual identities of the crystals used are supported, however, by their different colours, as well as by the paramagnetism of (2). Geometry parameters for (3) are given in Table 6.

The doubly deprotonated product, $\text{K}[\text{Re}(\text{o-pda})(\text{o-pbqd})_2]$, (4) which has two solvate thf molecules per complex, also has a structure for the anion with geometry very close to those of complex molecules (2) and (3). Geometry parameters are given in Table 7; a diagram of the unit cell constants is shown in Figure 6.

The molecular geometry of $\text{Re}(\text{abt})_3$ is shown in Figure 7. Selected bond lengths and angles are given in Table 8. The complex crystallises with one molecule in the asymmetric unit, and the molecular geometry also approximates trigonal prismatic, with the triangular faces defined by the three sulphur or three nitrogen atoms respectively. Following the convention of defining the distortion from trigonal prismatic by calculating the angles between the chelate planes and the triangular faces, twist angles of 4.5, 4.7, and 6.0° are obtained for ligands 1, 2, and 3 [associated with N(1), N(2), and N(3) respectively].

The carbon–carbon bond length patterns in the ligands show, as in $[\text{Re}(\text{o-pda})_3]^+$ and $\text{Re}(\text{o-pda})_3$, no apparent localisation of double bonds, indicating that the ligands are in the reduced form and that the metal is formally in the vi oxidation state.

Due to the different dimensions of the prism faces [the triangular face of sulphur atoms has longer sides (average S...S of 3.164 Å) than the triangle of nitrogen atoms (average N...N of 2.683 Å)], the trigonal prismatic geometry of the complex is distorted and the S_3N_3 polyhedron is severely tapered. Similar results were obtained for $\text{Tc}(\text{abt})_3$ and

Table 5. Bond lengths (\AA) and angles ($^\circ$) for compound (2)

Re–N(11)	1.997(8)	Re–N(12)	2.005(8)	C(23)–C(22)	1.400(12)	C(50)–C(40)	1.496(18)
Re–N(21)	2.001(8)	Re–N(22)	2.001(9)	C(23)–C(24)	1.386(14)	C(25)–C(24)	1.352(15)
Re–N(31)	1.998(8)	Re–N(32)	2.014(9)	C(26)–C(25)	1.403(15)	C(32)–C(31)	1.382(13)
C(11)–N(11)	1.381(11)	C(12)–N(12)	1.365(12)	C(36)–C(31)	1.417(13)	C(33)–C(32)	1.396(12)
C(21)–N(21)	1.345(11)	C(22)–N(22)	1.349(11)	C(34)–C(33)	1.369(15)	C(35)–C(34)	1.394(17)
C(31)–N(31)	1.362(11)	C(32)–N(32)	1.361(12)	C(36)–C(35)	1.330(17)	C(2)–O(1)	1.431(16)
C(12)–C(11)	1.385(13)	C(16)–C(11)	1.396(13)	C(4)–O(1)	1.437(14)	C(6)–C(2)	1.459(20)
C(13)–C(12)	1.414(13)	C(14)–C(13)	1.347(15)	C(5)–C(4)	1.522(20)	C(6)–C(5)	1.447(20)
C(15)–C(14)	1.416(16)	C(16)–C(15)	1.367(14)	C(20)–O(10)	1.432(15)	C(50)–O(10)	1.440(14)
C(22)–C(21)	1.402(12)	C(26)–C(21)	1.394(12)	C(30)–C(20)	1.525(19)	C(40)–C(30)	1.502(19)
N(12)–Re–N(11)	75.3(4)	N(21)–Re–N(11)	86.4(4)	C(16)–C(11)–N(11)	126.8(9)	C(16)–C(11)–C(12)	120.4(9)
N(21)–Re–N(12)	132.0(3)	N(22)–Re–N(11)	133.5(3)	C(11)–C(12)–N(12)	112.7(8)	C(13)–C(12)–N(12)	127.5(9)
N(22)–Re–N(12)	86.3(4)	N(22)–Re–N(21)	74.9(4)	C(13)–C(12)–C(11)	119.7(9)	C(14)–C(13)–C(12)	120.0(10)
N(31)–Re–N(11)	133.5(3)	N(31)–Re–N(12)	87.2(4)	C(15)–C(14)–C(13)	119.8(10)	C(16)–C(15)–C(14)	121.1(11)
N(31)–Re–N(21)	133.6(3)	N(31)–Re–N(22)	86.4(4)	C(15)–C(16)–C(11)	118.9(10)	C(32)–C(31)–N(31)	113.1(8)
N(32)–Re–N(11)	86.6(4)	N(32)–Re–N(12)	133.5(3)	C(36)–C(31)–N(31)	127.5(10)	C(36)–C(31)–C(32)	119.4(10)
N(32)–Re–N(21)	87.8(4)	N(32)–Re–N(22)	133.4(3)	C(31)–C(32)–N(32)	112.5(8)	C(33)–C(32)–N(32)	127.7(9)
N(32)–Re–N(31)	74.8(4)	C(11)–N(11)–Re	119.4(6)	C(33)–C(32)–C(31)	119.8(9)	C(34)–C(33)–C(32)	119.4(10)
C(12)–N(12)–Re	119.8(7)	C(21)–N(21)–Re	120.5(6)	C(35)–C(34)–C(33)	120.6(10)	C(36)–C(35)–C(34)	120.7(11)
C(22)–N(22)–Re	119.6(6)	C(31)–N(31)–Re	119.9(7)	C(35)–C(36)–C(31)	120.1(11)	C(4)–O(1)–C(2)	109.0(10)
C(32)–N(32)–Re	119.7(6)	C(22)–C(21)–N(21)	111.9(8)	C(6)–C(2)–O(1)	108.5(12)	C(5)–C(4)–O(1)	105.3(11)
C(26)–C(21)–N(21)	127.4(8)	C(26)–C(21)–C(22)	120.6(8)	C(6)–C(5)–C(4)	107.2(12)	C(5)–C(6)–C(2)	105.1(13)
C(21)–C(22)–N(22)	113.1(8)	C(23)–C(22)–N(22)	126.4(9)	C(50)–O(10)–C(20)	109.8(10)	C(30)–C(20)–O(10)	106.0(10)
C(23)–C(21)–C(21)	120.5(9)	C(25)–C(24)–C(23)	121.6(10)	C(40)–C(30)–C(20)	102.2(11)	C(50)–C(40)–C(30)	105.2(11)
C(24)–C(23)–C(22)	118.0(10)	C(26)–C(25)–C(24)	122.1(10)	C(40)–C(50)–O(10)	106.7(11)		
C(25)–C(26)–C(21)	117.3(9)	C(12)–C(11)–N(11)	112.8(8)				

Table 6. Bond lengths (\AA) and angles ($^\circ$) for compound (3)

N(11)–Re	2.023(12)	N(22)–Re	2.007(15)	C(24)–C(23)	1.375(23)	C(25)–C(24)	1.432(26)
N(21)–Re	2.003(13)	N(32)–Re	2.018(13)	C(26)–C(25)	1.390(25)	C(32)–C(31)	1.439(22)
N(31)–Re	1.993(14)	C(12)–N(12)	1.354(20)	C(36)–C(31)	1.434(24)	C(31)–C(32)	1.439(22)
C(11)–N(11)	1.395(19)	C(22)–N(22)	1.350(19)	C(33)–C(32)	1.425(21)	C(34)–C(33)	1.388(24)
C(21)–N(21)	1.359(19)	C(32)–N(32)	1.365(20)	C(35)–C(34)	1.396(26)	C(36)–C(35)	1.387(29)
C(31)–N(31)	1.366(20)	C(16)–C(11)	1.412(21)	C(1A)–O(1)	1.492(22)	C(4A)–O(1)	1.450(25)
C(12)–C(11)	1.410(21)	C(14)–C(13)	1.383(26)	C(2A)–C(1A)	1.489(30)	C(3A)–C(2A)	1.463(34)
C(13)–C(12)	1.437(22)	C(16)–C(15)	1.367(23)	C(4A)–C(3A)	1.528(34)	C(1B)–O(2)	1.437(21)
C(15)–C(14)	1.400(24)	C(26)–C(21)	1.456(22)	C(4B)–O(2)	1.448(22)	C(2B)–C(1B)	1.537(26)
C(22)–C(21)	1.427(21)	C(23)–C(22)	1.415(21)	C(3B)–C(2B)	1.488(28)	C(4B)–C(3B)	1.512(28)
N(12)–Re	2.008(13)						
N(11)–Re–N(31)	134.5(5)	N(11)–Re–N(32)	85.4(6)	C(26)–C(21)–N(21)	126.1(15)	C(26)–C(21)–C(22)	119.5(15)
N(11)–Re–N(21)	84.6(6)	N(11)–Re–N(22)	133.6(5)	C(21)–C(22)–N(22)	111.9(14)	C(23)–C(22)–N(22)	127.9(15)
N(12)–Re–N(31)	86.0(6)	N(12)–Re–N(32)	133.5(5)	C(23)–C(22)–C(21)	120.2(15)	C(24)–C(23)–C(22)	120.1(16)
N(12)–Re–N(21)	132.2(5)	N(12)–Re–N(22)	85.7(6)	C(25)–C(24)–C(23)	120.8(17)	C(26)–C(25)–C(24)	121.1(17)
N(12)–Re–N(11)	76.0(6)	N(21)–Re–N(31)	134.9(5)	C(25)–C(26)–C(21)	118.4(17)	C(32)–C(31)–N(31)	113.3(14)
N(21)–Re–N(32)	86.6(6)	N(22)–Re–N(31)	84.8(6)	C(36)–C(31)–N(31)	128.5(18)	C(36)–C(31)–C(32)	118.2(17)
N(22)–Re–N(32)	134.3(5)	N(22)–Re–N(21)	76.9(6)	C(31)–C(32)–N(32)	112.7(15)	C(33)–C(32)–N(32)	126.8(16)
N(32)–Re–N(31)	77.4(6)	C(11)–N(11)–Re	118.1(10)	C(33)–C(32)–C(31)	120.5(16)	C(34)–C(33)–C(32)	117.8(17)
C(12)–N(12)–Re	120.0(11)	C(21)–N(21)–Re	117.4(11)	C(35)–C(34)–C(33)	123.3(18)	C(36)–C(35)–C(34)	119.4(17)
C(22)–N(22)–Re	119.1(11)	C(31)–N(31)–Re	118.5(12)	C(35)–C(36)–C(31)	120.7(19)	C(4A)–O(1)–C(1A)	110.3(16)
C(32)–N(32)–Re	118.0(11)	C(12)–C(11)–N(11)	112.6(14)	C(2A)–C(1A)–O(1)	106.4(18)	C(3A)–C(2A)–C(1A)	105.7(21)
C(16)–C(11)–N(11)	125.6(15)	C(16)–C(11)–C(12)	121.7(16)	C(4A)–C(3A)–C(2A)	109.3(20)	C(3A)–C(4A)–O(1)	104.5(22)
C(11)–C(12)–N(12)	113.3(15)	C(13)–C(12)–N(12)	127.6(15)	C(4B)–O(2)–C(1B)	109.7(14)	C(2B)–C(1B)–O(2)	105.8(15)
C(13)–C(12)–C(11)	119.1(16)	C(14)–C(13)–C(12)	118.1(17)	C(3B)–C(2B)–C(1B)	103.5(17)	C(4B)–C(3B)–C(2B)	105.9(17)
C(15)–C(14)–C(13)	121.0(17)	C(16)–C(15)–C(14)	122.7(18)	C(3B)–C(4B)–O(2)	106.9(18)	C(21)–Re–C(32)	117.4(5)
C(15)–C(16)–C(11)	117.3(17)	C(22)–C(21)–N(21)	114.5(13)				

Mo(abt)_3 .^{3a,b} Furthermore, this tapered geometry may be a cause of a fairly large twist in the ligands to maximise metal *d* and ligand π_v orbital interactions.

The average Re–N distance of 2.00 \AA is comparable to that in $[\text{Re}(o\text{-pda})_3]^+$. As mentioned above, this short distance is indicative of a fair degree of multiple-bond character. The average Re–S distance is 2.343 \AA , compared to average Tc–S of 2.351 \AA in Tc(abt)_3 , where a significant degree of multiple-bond

character has been implied. Since the single-bond covalent radii of Re and Tc are similar, a fair amount of multiple bonding in the Re–S bond is indicated and hence a high degree of charge delocalisation over both ligand and metal. This would correlate well with e.s.r. studies of Re(abt)_3 ,^{3b} which showed that there was a high degree of electron delocalisation in the system, possibly via interaction of metal *d* and delocalised π_v ligand orbitals. The short, average N–C (1.34 \AA) and S–C (1.724 \AA)

Table 7. Bond lengths (\AA) and angles ($^\circ$) for compound (4)

N(12A)–Re(1A)	1.998(30)	N(11A)–Re(1A)	2.023(32)	C(31B)–N(31B)	1.400(45)	C(32B)–N(32B)	1.405(46)
N(22A)–Re(1A)	1.989(26)	N(21A)–Re(1A)	1.943(27)	C(12B)–C(11B)	1.417(40)	C(16B)–C(11B)	1.413(46)
N(31A)–Re(1A)	1.959(29)	N(32A)–Re(1A)	2.004(27)	C(13B)–C(12B)	1.400(47)	C(14B)–C(13B)	1.413(48)
C(12A)–N(12A)	1.414(49)	C(11A)–N(11A)	1.423(40)	C(15B)–C(14B)	1.343(52)	C(16B)–C(15B)	1.379(53)
C(22A)–N(22A)	1.428(41)	C(21A)–N(21A)	1.378(40)	C(22B)–C(21B)	1.450(39)	C(26B)–C(21B)	1.496(50)
C(31A)–N(31A)	1.395(50)	C(32A)–N(32A)	1.316(38)	C(23B)–C(22B)	1.418(46)	C(24B)–C(23B)	1.470(55)
C(12A)–C(11A)	1.378(47)	C(16A)–C(11A)	1.383(49)	C(25B)–C(24B)	1.435(53)	C(26B)–C(25B)	1.355(54)
C(13A)–C(12A)	1.392(45)	C(14A)–C(13A)	1.364(57)	C(32B)–C(31B)	1.531(46)	C(36B)–C(31B)	1.367(45)
C(15A)–C(14A)	1.459(59)	C(16A)–C(15A)	1.418(53)	C(33B)–C(32B)	1.389(55)	C(34B)–C(33B)	1.389(53)
C(22A)–C(21A)	1.389(55)	C(26A)–C(21A)	1.436(45)	C(35B)–C(34B)	1.421(50)	C(36B)–C(35B)	1.384(49)
C(23A)–C(22A)	1.437(49)	C(24A)–C(23A)	1.387(46)	C(11)–O(1)	1.443(57)	C(14)–O(1)	1.362(61)
C(25A)–C(24A)	1.391(47)	C(26A)–C(25A)	1.421(43)	C(12)–C(11)	1.692(76)	C(13)–C(12)	1.506(76)
C(32A)–C(31A)	1.398(49)	C(36A)–C(31A)	1.395(50)	C(14)–C(13)	1.507(77)	C(21)–O(2)	1.386(63)
C(33A)–C(32A)	1.553(55)	C(34A)–C(33A)	1.507(54)	C(24)–O(2)	1.390(69)	C(22)–C(21)	1.534(77)
C(35A)–C(34A)	1.429(62)	C(36A)–C(35A)	1.416(62)	C(23)–C(22)	1.532(74)	C(24)–C(23)	1.649(68)
N(11B)–Re(1B)	1.971(28)	N(12B)–Re(1B)	2.007(26)	C(31)–O(3)	1.433(79)	C(34)–O(3)	1.386(67)
N(21B)–Re(1B)	1.957(31)	N(22B)–Re(1B)	1.932(27)	C(32)–C(31)	1.50(11)	C(33)–C(32)	1.390(79)
N(31B)–Re(1B)	1.989(27)	N(32B)–Re(1B)	1.943(26)	C(34)–C(33)	1.390(79)	C(41)–O(4)	1.318(65)
C(11B)–N(11B)	1.382(39)	C(12B)–N(12B)	1.447(40)	C(44)–O(4)	1.487(58)	C(42)–C(41)	1.451(66)
C(21B)–N(21B)	1.353(43)	C(22B)–N(22B)	1.362(44)	C(43)–C(44)	1.546(66)	C(42)–C(43)	1.391(72)
N(11A)–Re(1A)–N(12A)	80.2(13)	N(22A)–Re(1A)–N(12A)	134.7(11)	N(32B)–Re(1B)–N(12B)	85.6(11)	N(32B)–Re(1B)–N(21B)	138.4(10)
N(22A)–Re(1A)–N(11A)	84.8(12)	N(21A)–Re(1A)–N(12A)	86.8(12)	N(32B)–Re(1B)–N(22B)	86.7(12)	N(32B)–Re(1B)–N(31B)	75.2(11)
N(21A)–Re(1A)–N(11A)	136.2(11)	N(21A)–Re(1A)–N(22A)	75.2(12)	C(11B)–N(11B)–Re(1B)	120.5(18)	C(12B)–N(12B)–Re(1B)	118.7(19)
N(31A)–Re(1A)–N(12A)	134.7(11)	N(31A)–Re(1A)–N(11A)	86.4(13)	C(21B)–N(21B)–Re(1B)	119.3(20)	C(22B)–N(22B)–Re(1B)	124.0(19)
N(31A)–Re(1A)–N(22A)	86.0(12)	N(31A)–Re(1A)–N(21A)	129.5(13)	C(31B)–N(31B)–Re(1B)	122.8(19)	C(32B)–N(32B)–Re(1B)	124.2(21)
N(32A)–Re(1A)–N(12A)	82.2(12)	N(32A)–Re(1A)–N(11A)	129.8(10)	C(12B)–C(11B)–N(11B)	114.0(26)	C(16B)–C(11B)–N(11B)	127.9(28)
N(32A)–Re(1A)–N(22A)	137.1(10)	N(32A)–Re(1A)–N(21A)	88.8(12)	C(16B)–C(11B)–C(12B)	117.3(28)	C(11B)–C(12B)–N(12B)	108.9(25)
N(32A)–Re(1A)–N(31A)	73.8(12)	C(12A)–N(12A)–Re(1A)	114.7(23)	C(13B)–C(12B)–N(12B)	130.3(27)	C(13B)–C(12B)–C(11B)	120.8(29)
C(11A)–N(11A)–Re(1A)	113.1(22)	C(22A)–N(22A)–Re(1A)	119.3(23)	C(14B)–C(13B)–C(12B)	119.2(30)	C(15B)–C(14B)–C(13B)	119.9(32)
C(21A)–N(21A)–Re(1A)	122.7(23)	C(31A)–N(31A)–Re(1A)	123.4(25)	C(16B)–C(15B)–C(14B)	121.9(35)	C(15B)–C(16B)–C(11B)	120.7(33)
C(32A)–N(32A)–Re(1A)	118.9(22)	C(12A)–C(11A)–N(11A)	115.6(30)	C(22B)–C(21B)–N(21B)	113.7(29)	C(26B)–C(21B)–N(21B)	129.1(27)
C(16A)–C(11A)–N(11A)	124.1(29)	C(16A)–C(11A)–C(12A)	120.2(28)	C(26B)–C(21B)–C(22B)	116.9(28)	C(21B)–C(22B)–N(22B)	107.0(26)
C(11A)–C(12A)–N(12A)	115.0(28)	C(13A)–C(12A)–N(12A)	126.9(33)	C(23B)–C(22B)–N(22B)	132.8(25)	C(23B)–C(22B)–C(21B)	120.1(30)
C(13A)–C(12A)–C(11A)	118.0(34)	C(14A)–C(13A)–C(12A)	123.2(34)	C(24B)–C(23B)–C(22B)	121.4(28)	C(25B)–C(24B)–C(23B)	117.3(35)
C(15A)–C(14A)–C(13A)	120.4(33)	C(16A)–C(15A)–C(14A)	114.2(37)	C(26B)–C(25B)–C(24B)	122.5(39)	C(25B)–C(26B)–C(21B)	121.6(30)
C(15A)–C(16A)–C(11A)	123.7(34)	C(22A)–C(21A)–N(21A)	111.1(30)	C(32B)–C(31B)–N(31B)	108.1(27)	C(36B)–C(31B)–N(31B)	130.1(26)
C(26A)–C(21A)–N(21A)	128.4(32)	C(26A)–C(21A)–C(22A)	119.0(30)	C(36B)–C(31B)–C(32B)	121.6(32)	C(31B)–C(32B)–N(32B)	107.9(30)
C(21A)–C(22A)–N(22A)	110.8(28)	C(23A)–C(22A)–N(22A)	123.4(34)	C(33B)–C(32B)–N(32B)	138.6(31)	C(33B)–C(32B)–C(31B)	113.5(32)
C(23A)–C(22A)–C(21A)	125.7(32)	C(24A)–C(23A)–C(22A)	112.4(34)	C(34B)–C(33B)–C(32B)	127.4(34)	C(35B)–C(34B)–C(33B)	113.6(35)
C(25A)–C(24A)–C(23A)	124.9(29)	C(26A)–C(25A)–C(24A)	121.6(28)	C(36B)–C(35B)–C(34B)	126.4(32)	C(35B)–C(36B)–C(31B)	117.4(30)
C(25A)–C(26A)–C(21A)	115.8(30)	C(32A)–C(31A)–N(31A)	105.6(29)	C(14)–O(1)–C(11)	112.7(35)	C(12)–C(11)–O(1)	102.4(37)
C(36A)–C(31A)–N(31A)	130.5(34)	C(36A)–C(31A)–C(32A)	123.8(36)	C(13)–C(12)–C(11)	102.6(41)	C(14)–C(13)–C(12)	107.3(46)
C(31A)–C(32A)–N(32A)	117.1(32)	C(33A)–C(32A)–N(32A)	123.8(36)	C(13)–C(14)–O(1)	110.8(40)	C(24)–O(2)–C(21)	114.4(39)
C(33A)–C(32A)–C(31A)	118.4(30)	C(34A)–C(33A)–C(32A)	115.3(33)	C(22)–C(21)–O(2)	112.4(44)	C(23)–C(22)–C(21)	101.6(41)
C(35A)–C(34A)–C(33A)	120.3(38)	C(36A)–C(35A)–C(34A)	121.1(37)	C(24)–C(23)–C(22)	107.2(40)	C(23)–C(24)–O(2)	102.9(39)
C(35A)–C(36A)–C(31A)	120.8(37)	N(12B)–Re(1B)–N(11B)	76.4(10)	C(34)–O(3)–C(31)	98.3(45)	C(32)–C(31)–O(3)	102.8(57)
N(21B)–Re(1B)–N(11B)	86.2(12)	N(12B)–Re(1B)–N(12B)	129.1(12)	C(33)–C(32)–C(31)	107.6(52)	C(34)–C(33)–C(32)	100.4(50)
N(22B)–Re(1B)–N(11B)	137.4(11)	N(22B)–Re(1B)–N(12B)	85.4(11)	C(33)–C(34)–O(3)	117.6(44)	C(44)–O(4)–C(41)	104.3(35)
N(22B)–Re(1B)–N(21B)	76.0(11)	N(31B)–Re(1B)–N(11B)	87.5(11)	C(42)–C(41)–O(4)	114.9(42)	C(43)–C(44)–O(4)	102.2(35)
N(31B)–Re(1B)–N(12B)	138.5(11)	N(31B)–Re(1B)–N(21B)	86.6(12)	C(42)–C(43)–C(44)	105.5(39)	C(43)–C(42)–C(41)	104.5(43)
N(31B)–Re(1B)–N(22B)	128.6(11)	N(32B)–Re(1B)–N(11B)	128.9(12)				

distances also agree with this model. The packing in the lattice is discussed later in connection with e.s.r. data.

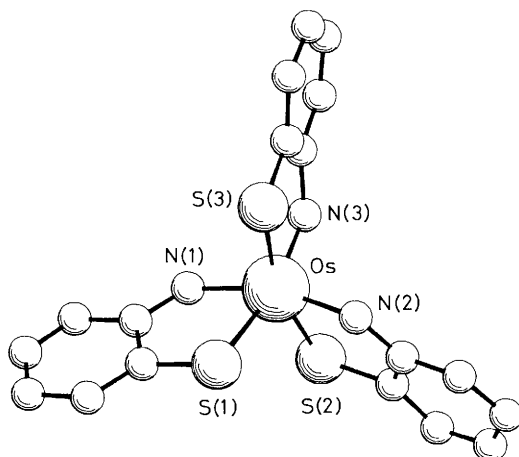
Summary. Assignment of metal oxidation states for complexes with unsaturated, chelating ligands, of the types discussed here, has always involved a fair degree of uncertainty and ambiguity due to the potential ‘non-innocent’ behaviour of these ligands towards internal redox reactions with the metal centres. Thus, a given oxidation state of a species may involve any one of a variety of combinations of metal and ligand oxidation states. In some, the dilemma is more obvious. For example, if $\text{V}(\text{S}_2\text{C}_2\text{Ph}_2)_3$ ²² were to involve dianionic ligands the metal oxidation state would be vi. This is clearly unlikely, since it would involve breaking into the $3p^6$ closed shell of the metal; molecular orbital calculations for $\text{M}(\text{S}_2\text{C}_2\text{Ph}_2)_3$ ($\text{M} = \text{Re}, \text{W}$, or Mo) have led to the suggestions of limiting oxidation-state

formulations for the metals of ii and vi,⁴ although a favoured formulation could not be determined.

From the present spectroscopic and chemical evidence there is justification in the assignment of an oxidation state of vii to the rhenium in the $[\text{Re}(\text{o-pda})_3]^+$ ion. First, in the ^1H n.m.r. spectrum, the coupling constants for the ring protons indicate aromaticity in the ligands, consistent with the reduced, dianionic, ligand form, with consequently the metal in the vii oxidation state. Interaction of metal d_{xy} and $d_{x^2-y^2}$ orbitals with delocalised, ligand π_v orbitals is believed to be an important stabilising factor in this geometry.^{7,16} Thus, compatibility of these orbitals is important, and as the metal d orbitals are destabilised as one moves from right to left in the Periodic Table, the tendency towards trigonal prismatic geometry decreases. Calculations have also indicated that, electronically,

Table 8. Bond lengths (Å) and angles (°) for compound (**5**)

S(1)-Re	2.329(7)	S(2)-Re	2.357(7)	C(15)-C(14)	1.311(31)	C(16)-C(15)	1.402(25)
S(3)-Re	2.343(7)	N(1)-Re	2.005(16)	C(22)-C(21)	1.395(29)	C(26)-C(21)	1.402(29)
N(2)-Re	1.994(16)	N(3)-Re	2.003(16)	C(23)-C(22)	1.349(28)	C(24)-C(23)	1.430(27)
C(11)-S(1)	1.721(24)	C(21)-S(2)	1.754(25)	C(25)-C(24)	1.306(25)	C(26)-C(25)	1.414(25)
C(31)-S(3)	1.697(23)	C(16)-N(1)	1.348(22)	C(32)-C(31)	1.381(27)	C(36)-C(31)	1.426(29)
C(26)-N(2)	1.319(21)	C(36)-N(3)	1.354(22)	C(33)-C(32)	1.424(32)	C(34)-C(33)	1.314(34)
C(12)-C(11)	1.433(27)	C(16)-C(11)	1.410(27)	C(35)-C(34)	1.389(28)	C(36)-C(35)	1.396(24)
C(13)-C(12)	1.394(33)	C(14)-C(13)	1.439(33)				
S(2)-Re-S(1)	85.0(3)	S(3)-Re-S(1)	84.2(3)	C(15)-C(14)-C(13)	122.6(24)	C(16)-C(15)-C(14)	119.2(24)
S(3)-Re-S(2)	85.5(3)	N(1)-Re-S(1)	79.4(6)	C(11)-C(16)-N(1)	116.8(21)	C(15)-C(16)-N(1)	122.5(22)
N(1)-Re-S(2)	140.2(5)	N(1)-Re-S(3)	128.3(6)	C(15)-C(16)-C(11)	120.7(20)	C(22)-C(21)-S(2)	122.5(19)
N(2)-Re-S(1)	129.0(5)	N(2)-Re-S(2)	77.4(6)	C(26)-C(21)-S(2)	114.5(17)	C(26)-C(21)-C(22)	122.9(22)
N(2)-Re-S(3)	139.9(5)	N(2)-Re-N(1)	84.6(7)	C(23)-C(22)-C(21)	116.5(25)	C(24)-C(23)-C(22)	121.4(24)
N(3)-Re-S(1)	140.3(5)	N(3)-Re-S(2)	128.2(6)	C(25)-C(24)-C(23)	121.4(23)	C(26)-C(25)-C(24)	120.0(22)
N(3)-Re-S(3)	78.4(7)	N(3)-Re-N(1)	83.9(8)	C(21)-C(26)-N(2)	115.7(20)	C(25)-C(26)-N(2)	126.7(24)
N(3)-Re-N(2)	84.2(7)	C(11)-S(1)-Re	102.5(9)	C(25)-C(26)-C(21)	117.6(20)	C(32)-C(31)-S(3)	125.4(21)
C(21)-S(2)-Re	101.9(8)	C(31)-S(3)-Re	102.9(9)	C(36)-C(31)-S(3)	116.3(14)	C(36)-C(31)-C(32)	118.1(21)
C(16)-N(1)-Re	125.9(15)	C(26)-N(2)-Re	129.7(16)	C(33)-C(32)-C(31)	119.5(25)	C(34)-C(33)-C(32)	118.6(25)
C(36)-N(3)-Re	127.5(16)	C(12)-C(11)-S(1)	124.0(19)	C(35)-C(34)-C(33)	126.8(27)	C(36)-C(35)-C(34)	114.0(23)
C(16)-C(11)-S(1)	115.4(19)	C(16)-C(11)-C(12)	120.4(23)	C(31)-C(36)-N(3)	114.7(18)	C(35)-C(36)-N(3)	122.5(21)
C(13)-C(12)-C(11)	116.5(24)	C(14)-C(13)-C(12)	120.4(22)	C(35)-C(36)-C(31)	122.5(19)		

**Figure 8.** The molecular structure of Os(abt)₃.

the optimum situation for this geometry involves low numbers of *d* electrons, especially *d*⁰-*d*² system.¹⁸ Therefore, the near-perfect trigonal prismatic geometry in [Re(*o*-pda)₃]⁺ would tend to agree with a rhenium(vii) *d*⁰ species.

The carbon–carbon bond patterns within the ligand rings are also more in keeping with the delocalised π -bonding system in the reduced, phenylenediamido form than with the localised double-bond structure of the di-imino form of the ligand.

The deprotonation of [Re(*o*-pda)₃]⁺ is also rationalised more easily with respect to a rhenium(vii) species with dianionic, *o*-phenylenediamido ligands.

Finally, the reversible reduction of [Re(*o*-pda)₃]⁺ to the paramagnetic Re(*o*-pda)₃ provides evidence for the VII oxidation state of the cation.

Osmium Compounds.—Aminobenzenethiolate. The osmium-(vi) complex, Os(abt)₃ (**6**), was obtained by the reaction of OsO₄ with excess of *o*-aminobenzenethiol in THF in the presence of molecular sieves, in high yield as air-stable, deep red, rhombooidal plates. Like Re(abt)₃, the compound is very soluble in organic solvents, giving deep red solutions, and gives an acetone solvate.

The diamagnetic compound is a non-electrolyte in MeCN. The i.r. spectrum has bands at 3 231 and 1 543 cm⁻¹, assigned to v(N–H) and v(C=C) respectively, by comparison with Re(abt)₃; there are also strong bands at 565 and 386 cm⁻¹, which may be assigned to v(OsN) and tentatively to v(Os–S)¹¹ respectively.

The ¹H n.m.r. spectrum consists of a broad resonance at δ 12.22(1) ($\Delta_{\frac{1}{2}} = 27$ Hz), assigned to the NH protons. There is also a fairly well resolved ABCD splitting pattern, assigned to the aromatic protons, of two sets of multiplets (each comprising of a triplet in between two doublets) at δ 6.86(1) and 7.02(1) (H_B, H_C; separation of outer lines ca. 17 Hz) and two doublets of doublets at δ 7.57(1) and 7.59(1) (H_A, H_D; $J_{AB} = J_{CD} = 5$ Hz).

The structure of compound (**6**), as an acetone solvate, has been determined. A diagram of the molecule is shown in Figure 8; bond lengths and angles are given in Table 9. The development and refinement of the structure was complicated by pseudo-symmetry problems (see Experimental section). Thus atoms S(2), S(3), N(1), N(2), and Os are approximately coplanar and perpendicular to the *c* axis (the space group is *Pna*2₁) whilst N(3) and S(1) are approximately related by the pseudo-mirror. Nevertheless, the structure is reasonably well defined. The molecular geometry is best described as a distorted octahedron with the distortions arising both from the restricted chelate bites (S–Os–N angles are 79–82°) and a tendency towards a trigonal prismatic geometry. The arrangement of the S₃N₃ co-ordination set is meridional and so the two trigonal planes approximately perpendicular to the pseudo-three-fold axis of the tris chelate propeller are N₂S and S₂N. This arrangement will be expected to introduce some deviation from ideal, symmetrical structure.

With this unsymmetrical arrangement of co-ordinating atoms it becomes difficult to decide how to define the pseudo-three-fold axis commonly used as a reference axis for octahedral and trigonal prismatic structure comparisons as discussed above. After detailed consideration of this problem it occurred to us that a simple method of testing for twist distortions, rather than chelating asymmetry (e.g. due to different atom types and thus bond lengths), and chelate bite restrictions, as here, is to calculate the angles between the three chelate planes (or more rigorously, their perpendiculars). In this case, a true octahedral tris chelate (including distortions due to bite, etc.) will give three angles of 90°, a trigonal prism three angles of 120°. Intermediate

Table 9. Bond lengths (Å) and angles (°) for compound (**6**)

S(1)-Os	2.366(9)	S(2)-Os	2.354(8)	C(8)-C(7)	1.382(30)	C(12)-C(7)	1.389(34)
S(3)-Os	2.331(9)	N(1)-Os	2.018(20)	C(9)-C(8)	1.456(34)	C(10)-C(9)	1.414(34)
N(2)-Os	1.961(21)	N(3)-Os	1.935(46)	C(11)-C(10)	1.363(38)	C(12)-C(11)	1.357(41)
C(1)-S(1)	1.697(27)	C(7)-S(2)	1.747(24)	C(14)-C(13)	1.390(38)	C(18)-C(13)	1.429(41)
C(13)-S(3)	1.720(31)	C(2)-N(1)	1.295(31)	C(15)-C(14)	1.421(41)	C(16)-C(15)	1.317(47)
C(8)-N(2)	1.344(29)	C(14)-N(3)	1.398(44)	C(17)-C(16)	1.425(56)	C(18)-C(17)	1.383(57)
C(2)-C(1)	1.476(33)	C(6)-C(1)	1.378(35)	C(20)-C(19)	1.532(58)	C(21)-C(19)	1.569(69)
C(3)-C(2)	1.398(38)	C(4)-C(3)	1.318(42)	O(2)-C(19)	1.282(61)		
C(5)-C(4)	1.354(56)	C(6)-C(5)	1.397(45)				
S(2)-Os-S(1)	100.5(4)	S(3)-Os-S(1)	91.4(3)	C(5)-C(4)-C(3)	127.0(42)	C(6)-C(5)-C(4)	117.2(30)
S(3)-Os-S(2)	162.9(3)	N(1)-Os-S(1)	79.2(6)	C(5)-C(6)-C(1)	120.1(25)	C(8)-C(7)-S(2)	115.1(16)
N(1)-Os-S(2)	91.2(6)	N(1)-Os-S(3)	103.2(6)	C(12)-C(7)-S(2)	123.0(21)	C(12)-C(7)-C(8)	121.9(21)
N(2)-Os-S(1)	87.9(17)	N(2)-Os-S(2)	79.8(6)	C(7)-C(8)-N(2)	118.1(20)	C(9)-C(8)-N(2)	121.8(22)
N(2)-Os-S(3)	88.5(8)	N(2)-Os-N(1)	162.7(16)	C(9)-C(8)-C(7)	119.9(19)	C(10)-C(9)-C(8)	114.6(25)
N(3)-Os-S(1)	166.3(10)	N(3)-Os-S(2)	88.3(11)	C(11)-C(10)-C(9)	121.1(24)	C(12)-C(11)-C(10)	122.5(26)
N(3)-Os-S(3)	82.3(11)	N(3)-Os-N(1)	90.4(13)	C(11)-C(12)-C(7)	117.8(31)	C(14)-C(13)-S(3)	118.3(21)
N(3)-Os-N(2)	104.0(21)	C(1)-S(1)-Os	101.7(9)	C(18)-C(13)-S(3)	121.9(25)	C(18)-C(13)-C(14)	119.7(30)
C(7)-S(2)-Os	100.6(8)	C(13)-S(3)-Os	99.1(10)	C(13)-C(14)-N(3)	115.2(30)	C(15)-C(14)-N(3)	124.4(29)
C(2)-N(1)-Os	127.3(16)	C(8)-N(2)-Os	126.4(15)	C(15)-C(14)-C(13)	119.6(28)	C(16)-C(15)-C(14)	122.3(34)
C(14)-N(3)-Os	124.0(27)	C(2)-C(1)-S(1)	115.8(19)	C(17)-C(16)-C(15)	118.2(38)	C(18)-C(17)-C(16)	123.0(41)
C(6)-C(1)-S(1)	124.7(20)	C(6)-C(1)-C(2)	119.4(23)	C(17)-C(18)-C(13)	117.1(31)	C(21)-C(19)-C(20)	116.1(49)
C(1)-C(2)-N(1)	116.0(22)	C(3)-C(2)-N(1)	126.7(23)	O(2)-C(19)-C(20)	118.6(48)	O(2)-C(19)-C(21)	125.3(44)
C(3)-C(2)-C(1)	117.4(23)	C(4)-C(3)-C(2)	118.5(33)				

values will therefore be a pointer to an intermediate configuration and a spread of values a pointer to more general distortions. In the case of Os(abt)₃, the three angles are 100.0, 102.8, and 105.7°, indicating some movement from octahedral towards trigonal prismatic and some small additional distortion.

This distortion from the octahedral may thus account for its diamagnetism noted also for the analogous catechol complexes.^{9a,b}

Using the interplanar angle calculation for Re(abt)₃, values of 118.6–119.7° are obtained, which highlight the small degree of twist from trigonal prismatic indicated by the previous ‘twist angle’ calculation (see earlier).

As in the trigonal prismatic complexes described above, there is no obvious pattern in the carbon–carbon bond lengths within the ligand rings and this is taken to indicate aromaticity in the rings, associated with the reduced form of the ligand. The oxidised form would contain localised double bonds.

The average N–C and S–C bond lengths of 1.346 and 1.721 Å respectively compare quite well with those in Re(abt)₃ (averages N–C, 1.34 Å; S–C, 1.724 Å). This may indicate, as in the case of Re(abt)₃, that there is some degree of π character in these bonds.

The average Os–N bond length is 1.97 Å. As the single-bond covalent radius of Os is *ca.* 0.02 Å less than that of Re, this suggests similar multiple-bond character in the Os–N bonds, but the average Os–S distance of 2.35 Å, compared to the average Re–S distance of 2.343 Å in Re(abt)₃, indicates less multiple-bond character.

trans-OsO₂(*o*-pda)₂. The reaction of OsO₄ with a slight excess of *o*-phenylenediamine in thf in the presence of molecular sieves gave a moderate yield of a brown, air-stable solid of relatively low solubility in polar organic solvents. The compound formulated as OsO₂(*o*-pda)₂ (**7**) is diamagnetic and a non-electrolyte in thf. This is similar to the catecholates *trans*-OsO₂(cat)L₂, L = pyridine or substituted pyridine, obtained by reaction of OsO₄ with catechols in the presence of pyridine or substituted pyridine.^{9a} The reaction of *cis*-[OsO₄(OH)₂]²⁻ or *trans*-[OsO₂(OH)₄]²⁻ with catechols (H₂cat) also gave *trans*-[OsO₂(cat)₂]²⁻.^{9a}

The compound analysed quite well for N and H, but the C analysis is less satisfactory as is commonly found for osmium compounds.¹¹ The i.r. spectrum has bands at 3 312, 3 298, and

3 277 cm⁻¹, assigned to v(N–H). This multiplicity is most likely due to solid-state effects, as found in M[*o*-(HN)₂C₆H₄]₂ (M = Co, Ni, Pd, or Pt),² which all show a triplet of N–H stretches in the i.r. region. Bands at 1 584 and 574 cm⁻¹ can be assigned to v(C=C) and v(Os–N), respectively, and a very strong band at 865 cm⁻¹ to v(Os=O). The latter compares well with v(Os=O) of complexes containing the *trans*-O=Os=O ‘osmyl’ group;²³ there is also a weak band at 340 cm⁻¹, not seen for Os(abt)₃, which may be due to the deformation mode of the osmyl group, δ(OsO₂).^{9a}

The ¹H n.m.r. spectrum shows a fairly broad singlet at δ 10.42(1), assigned to the NH protons. The aromatic proton resonances give rise to an AA'BB' splitting pattern, consisting of two sextets at δ 6.94(1) (H_A, H_{A'}; separation of outer lines 17 Hz) and 6.56(1) (H_B, H_{B'}; separation of outer lines 17 Hz). This again agrees with a *trans*-O=Os=O structure, since a *cis* arrangement would result in inequivalent NH groups and an ABCD splitting pattern.

The complex OsO₂(*o*-pda)₂ is formally an osmium(viii) species. Thus for both Re and Os, *o*-aminobenzenethiol seems to give complexes in lower metal oxidation states than does *o*-phenylenediamine. Toluene-3,4-dithiolate(tdt) and *cis*-1,2-dicyanoethylene-1,2-dithiolate(mnt) ligands also show tendencies to stabilise oxidised and reduced forms of 1,2-dithiolene complexes respectively.¹¹

Spectroscopic and Electrochemical Data.—Electronic spectra. The electronic absorption data for the *o*-phenylenediamido and *o*-aminobenzenethiolato complexes are given in Table 10. For the complexes with trigonal prismatic geometries {i.e. [Re(*o*-pda)₃][ReO₄], [Re(*o*-pda)₃]PF₆, Re(*o*-pda)₃, and Re(abt)₃} there are three common bands, a high-intensity band at *ca.* 660 nm, a medium-intensity shoulder at *ca.* 420 nm, and a band at around 370 nm, the intensity of which is usually between those of the first two bands. This pattern agrees quite well with that observed for the series M(S₂C₂Ph₂)₃ (M = Mo, W, or Re) and M(tdt)₃ (M = Mo, W, or Re), where common bands at *ca.* 670 and 420 nm were observed.⁴ The geometries of many members of this series are known to be trigonal prismatic, *i.e.* Re(S₂C₂Ph₂)₃,^{19a} Mo(S₂C₂Ph₂)₃,^{19b} Re(tdt)₃,^{7b} and W(S₂C₂Ph₂)₃.^{7a,b}

Table 10. Electronic spectra for complexes of rhenium and osmium in MeCN

Compound	Maxima ^a						
	ν_1	ν_2	ν_3	ν_4	ν_5	ν_6	ν_7
[Re(<i>o</i> -pda) ₃][ReO ₄] ^b	666 (3.4)			419 ^c (1.5)	380 (1.8)	274 (2.3)	
[Re(<i>o</i> -pda) ₃]PF ₆ ^b	666 (3.0)			408 ^c (1.3)	376 (1.5)		
Re(<i>o</i> -pda) ₃	646 (9.0)	553 (9.6)		412 ^c (6.5)	384 ^c (8.5)	342 (13.2)	
Re(<i>o</i> -pda) ₂ (<i>o</i> -pbqd)		504 (0.9)			360 (1.9)	286 (2.3)	
K[Re(<i>o</i> -pda)(<i>o</i> -pbqd) ₂]			494 ^c (0.7)		364 (1.9)	294 (2.7)	
Re(abt) ₃ ^b	680 ^c (0.5)	586 (0.8)		452 ^c (0.2)	354 (1.2)	300 (0.7)	
Os(abt) ₃ ^d		538 ^c (1.1)	456 (1.5)	416 ^c (1.1)	332 (1.2)		
OsO ₂ (<i>o</i> -pda) ₂					337 (2.3)	288 (1.5)	244 (0.8)

^a Values in nm, with $10^4 \epsilon / \text{dm}^3 \text{ mol}^{-1} \text{ cm}^{-1}$ in parentheses. ^b Trigonal prismatic geometry. ^c Shoulder. ^d Severely distorted geometry (see text).

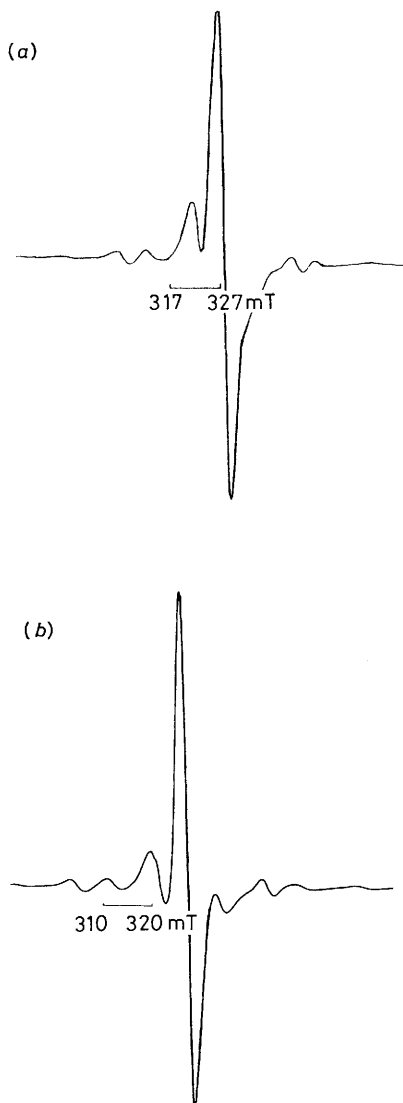


Figure 9. E.s.r. spectra in frozen thf solution of (a) Re(abt)₃ and (b) Re(*o*-pda)₃ at 77 K

Thus, similarities in the electronic spectral properties of these 'dithiolene' type complexes add further evidence of similarities in their electronic structures, and give indications of similarities in their molecular geometries.

The spectrum of Os(abt)₃ is very different to those of the trigonal prismatic complexes as expected from its distorted octahedral geometry. Similarly, the deprotonation products, Re(*o*-pda)₂(*o*-pbqd) and K[Re(*o*-pda)(*o*-pbqd)₂], have spectra quite different to those of the other trigonal prismatic complexes. Differences in spectral properties need not necessarily imply structural differences and as another example [AsPh₄]₂[Mo(mnt)₃] and [AsPh₄]₂[W(mnt)₃] have similar structures but very different electronic absorption spectra.²⁴ One possible explanation is that in these anionic complexes the electronic transitions are more metal related than in the neutral complexes.

E.s.r. spectra. The spectra of both Re(*o*-pda)₃ and Re(abt)₃ in frozen thf solution are shown in Figure 9. For Re(*o*-pda)₃ there is a central isotropic line at $g = 2.008$ with a peak-to-peak width of 3 mT. At 7.5 mT on either side there are shoulders 15 mT apart with isotropic g (2.008) and hyperfine ($A_{\text{iso}} = 3$ mT) values, whilst further out there are weak satellites equally spaced at 16.5, 24.0, and 35.5 mT on either side of the central line.

The spectrum of Re(abt)₃ under the same conditions is very similar with a central isotropic line at $g = 2.012$ (width 3.13 mT), shoulders at 5.8 and 11.6 mT apart, with weak satellites further out at 16.5, 21.0, and 33.5 mT either side of the central line. This spectrum of Re(abt)₃ shows some features of the solvent- and concentration-dependent spectra reported by Baldas *et al.*^{3b} who used EtOH, CHCl₃, pyridine, C₆H₆, dimethyl formamide, dimethyl sulphoxide, and MeCN as solvents, and concluded that (a) there is extensive delocalisation of electron spin on to the abt ligands, (b) there is some type of polymerisation in solution with intermolecular interactions between molecules in solution, and (c) the weaker features were due to a monomeric species. The central line was always interpreted as due to a polymeric species and they made the assumption that 'Re(abt)₃ is isomorphous with Mo(abt)₃ and Tc(abt)₃ and that the molecular arrangements in solution are similar to those in the crystalline solid state.'

In view of this proposal by Baldas *et al.* it is pertinent to examine in detail the solid-state structure of Re(abt)₃, in order to identify any possible intermolecular interactions. Baldas *et al.* postulated interactions between ligands, and this is not so unrealistic, considering the proposal that the unpaired electron

Table 11. Cyclic voltammetry data for complexes of rhenium and osmium^a

Compound	<i>E</i> (4+/5+)	<i>E</i> (5+/6+)	<i>E</i> (6+/7+)	<i>E</i> (7+/8+)
[Re(<i>o</i> -pda) ₃]PF ₆ ^b		-0.92	-0.53	
Re(<i>o</i> -pda) ₃ ^c		-0.96	-0.56	
Os(abt) ₃ ^d	-1.50	-0.825	-0.10	-0.485

^a In MeCN solutions with 0.2 mol dm⁻³ NBu₄PF₆ as inert electrolyte. Potentials (V) are given vs. *E*(for ferrocene–ferrocenium) = 0.00 V (under the experimental conditions, average *E* = +0.46 V, ΔE_v = 80 mV). Scan rate 100 mV s⁻¹. ^b Data correspond to two reversible reductions. There is an additional irreversible oxidation at +0.45 V. ^c Data correspond to one reversible oxidation and one reversible reduction. There is an additional irreversible oxidation at +0.43 V. ^d Data correspond to two reversible oxidations and two reversible reductions.

Table 12. Crystal data, details of intensity measurements, and structure refinement

Compound	(1)	(2)	(3)	(4)	(5)	(6)
Formula	C ₂₄ H ₁₈ N ₆ O ₄ Re ₂ ·C ₃ H ₆ O	C ₁₈ H ₁₈ N ₆ Re·2C ₄ H ₈ O	C ₁₈ H ₁₇ N ₆ Re·2C ₄ H ₈ O	C ₁₈ H ₁₆ KN ₆ Re·2C ₄ H ₈ O	C ₁₈ H ₁₅ N ₃ ReS ₃	C ₁₈ H ₁₅ N ₃ OsS ₃ ·C ₃ H ₆ O
<i>M</i>	884.92	648.792	647.784	685.876	555.71	617.79
Crystal system	Triclinic	Orthorhombic	Orthorhombic	Monoclinic	Orthorhombic	Orthorhombic
<i>a</i> /Å	12.417	9.206(8)	9.194(2)	17.147(3)	10.664	15.095(4)
<i>b</i> /Å	19.873	16.677(3)	16.672(2)	14.441(3)	11.356	9.740(1)
<i>c</i> /Å	10.585	16.814(2)	16.818(2)	21.999(3)	15.221	15.229(5)
$\alpha/^\circ$	81.22	90.0	90.0	90.0	90.0	90
$\beta/^\circ$	102.21	90.0	90.0	92.25(1)	90.0	90
$\gamma/^\circ$	83.17	90.0	90.0	90.0	90.0	90
<i>U</i> /Å ³	2 491.88	2 581.43	2 577.90	5 443.18	1 843.27	2 239.05
Space group	<i>P</i> ī	<i>P</i> 2 ₁ 2 ₁ 2 ₁	<i>P</i> 2 ₁ 2 ₁ 2 ₁	<i>C</i> c	<i>P</i> 2 ₁ 2 ₁ 2 ₁	<i>P</i> na2 ₁
<i>Z</i>	4	4	4	8	4	4
<i>D</i> _c /g cm ⁻³	2.358	1.669	1.66	1.673	2.002	1.832
μ/cm^{-1}	98.54	47.75	44.88	46.73	69.80	57.30
<i>F</i> (000)	1 672	1 291	1 288	2 720	1 068	1 092
Crystal size (mm)	0.38 × 0.48 × 0.63	0.43 × 0.13 × 0.10	0.7 × 0.38 × 0.2	0.55 × 0.25 × 0.1	0.33 × 0.15 × 0.25	0.8 × 0.3 × 0.23
Max., min. transmission	1.0, 0.80	1.0, 0.75	1.0, 0.34	1.0, 0.38	1.0, 0.67	1.0, 0.78
<i>h</i> , <i>k</i> , <i>l</i> range	-14 to 14 -23 to 23 0-12	0-10 0-19 0-20	0-10 0-19 0-20	0-20 0-17 -26 to 26	0-12 0-13 0-18	0-11 0-17 0-18
Total no. of reflections	9 291	2 602	2 595	5 248	1 884	2 266
No. of unique reflections	8 766	2 579	2 572	5 024	1 863	2 045
No. of reflections used	3 903	2 345	1 744	2 896	1 229	1 517
[<i>F</i> > 3σ(<i>F</i>)]						
No. of parameters	452	334	316	502	232	237
Weighting scheme	0.001 286	0.000 854	0.000 396	0.000 978	0.000 237	0.000 609
parameter <i>g</i> in <i>w</i> = 1/[σ ² (<i>F</i>) + <i>gF</i> ₀ ²]						
Final <i>R</i> *	0.0561	0.0240	0.0365	0.0587	0.0462	0.0402
Final <i>R'</i>	0.0566	0.0254	0.0346	0.0583	0.0357	0.0402

* The absolute structures for compounds (2)–(6) were determined by use of the UNDO-1 facility in SHELX 76.

is delocalised into the ligand system. However, face-to-face interactions (the so-called ‘graphitic stacking’) are not a strong feature of the structure, partly due to the absence of centres of symmetry in the structure (the space group is *P*2₁2₁2₁). There are, however, a small number of ‘oblique’ C···C contacts, close to the limits normally used for normal C···C close packing, 3.4–3.5 Å, at 3.39–3.47 Å, but it is debatable whether these correspond to ‘electron interaction routes.’ In square planar metal dithiolates containing columnar stacking, or compounds with similar sulphur-containing ligands, where electronic interactions are demonstrably present in the solid state, those are believed to occur via S···S interactions. Accordingly we also looked at the S···S intermolecular contacts in our structure, but none was found below 4.0 Å. We therefore must conclude that our structure presents no evidence for significant interactions in the solid state which might support the ideas of association in solutions.

For both Re(*o*-pda)₃ and Re(abt)₃ which are very soluble in organic solvents it is thus far from clear how chemical bonding interaction could lead to polymerisation in very dilute (10⁻⁵ mol dm⁻³) solution. The spectra can possibly be explained as those

of only monomeric species in either case, with extensive delocalisation of the electron spin on to the ligands giving rise to the central isotropic peak. For other rhenium(vi) compounds with octahedral or tetrahedral geometries, the single unpaired electron gives rise to a six-line hyperfine structure (due to Re^{185,187}, *I* = 5/2).^{8,25} Note that for the tris catecholate complexes,⁸ Re(cat)₃, cat = C₁₄H₂₀O₂ and C₆Cl₄O₂, as for Re(abt)₃, the distance between the rhenium atoms is *ca.* 9 Å, and that strong intermolecular exchange is regarded as unlikely, especially in view of the six-line hyperfine e.s.r. spectrum which could be observed even at room temperature indicating electron spin density uniquely on the metal atom. The weak additional bands of Re(*o*-pda)₃ and Re(abt)₃ could hence arise from the time the electron actually spends on the rhenium centre. This would not explain the apparent concentration dependence however; it is possible that traces of oxygen in the dilute solutions of these air-sensitive compounds, or in the studies of Baldas *et al.* reaction with the solvents, may be responsible. It may be noted that on exposure to air the e.s.r. spectrum of Re[(HN)₂C₆H₄]₃ in thf disappears and the solution becomes green due to oxidation to diamagnetic Re(*o*-pda)₃⁺.

Table 13. Fractional atomic co-ordinates ($\times 10^4$) for compound (1)

Atom	<i>x</i>	<i>y</i>	<i>z</i>	Atom	<i>x</i>	<i>y</i>	<i>z</i>
Re(1)	6 774.2(9)	1 481.6(5)	1 228.9(10)	C(3B)	9 855(24)	7 644(13)	6 648(27)
Re(2)	7 434.2(10)	6 563.8(5)	4 662.9(10)	C(4B)	10 475(25)	8 091(15)	6 124(31)
N(11)	5 144(16)	1 594(10)	544(19)	C(5B)	10 376(27)	8 268(16)	4 747(33)
N(12)	6 625(17)	830(10)	-69(18)	C(6B)	9 728(25)	7 971(14)	3 927(28)
N(13)	6 457(18)	1 434(10)	3 009(19)	C(7B)	5 162(22)	7 153(12)	3 565(25)
N(14)	7 912(19)	713(11)	2 323(22)	C(8B)	4 043(31)	7 458(15)	2 622(29)
N(15)	7 989(18)	1 787(10)	422(20)	C(9B)	3 142(31)	7 575(18)	3 094(34)
N(16)	6 541(16)	2 511(10)	1 141(19)	C(10B)	3 204(26)	7 337(15)	4 465(30)
N(21)	8 409(18)	6 916(10)	6 079(20)	C(11B)	4 206(25)	7 070(14)	5 352(28)
N(22)	8 309(18)	7 169(11)	3 740(29)	C(12B)	5 167(23)	6 979(12)	4 921(25)
N(23)	6 168(18)	6 746(11)	5 538(20)	C(13B)	8 257(26)	5 069(16)	5 502(32)
N(24)	6 082(18)	7 012(11)	3 216(19)	C(14B)	8 189(27)	5 261(15)	4 140(30)
N(25)	7 741(20)	5 892(13)	3 500(24)	C(15B)	8 510(30)	4 693(19)	3 516(35)
N(26)	7 864(22)	5 646(12)	5 943(23)	C(16B)	8 943(32)	4 054(20)	4 264(38)
C(1A)	5 606(20)	819(12)	-755(21)	C(17B)	8 914(28)	3 886(17)	5 559(35)
C(2A)	4 722(21)	1 239(11)	-442(22)	C(18B)	8 566(28)	4 414(17)	6 264(33)
C(3A)	5 358(23)	377(14)	-1 675(27)	Re(3)	3 107.6(11)	3 556.7(6)	339.1(11)
C(4A)	4 297(26)	424(14)	-2 321(27)	O(10)	2 935(17)	2 962(10)	-644(19)
C(5A)	3 409(25)	864(15)	-2 034(30)	O(20)	2 676(20)	4 337(11)	-693(21)
C(6A)	3 606(22)	1 299(13)	-1 119(24)	O(30)	4 484(20)	3 417(11)	1 114(23)
C(7A)	7 073(20)	974(12)	4 028(23)	O(40)	2 284(16)	3 468(10)	1 481(18)
C(8A)	7 907(19)	533(12)	3 631(23)	C(10A)	5 624(32)	4 967(19)	7 452(35)
C(9A)	8 561(21)	-6(12)	4 511(26)	C(20A)	4 581(41)	5 171(26)	7 858(47)
C(10A)	8 522(24)	-94(14)	5 842(27)	C(30A)	5 750(46)	4 293(30)	7 041(52)
C(11A)	7 701(26)	349(15)	6 256(28)	O(10A)	6 428(20)	5 243(11)	7 719(22)
C(12A)	6 959(23)	828(13)	5 361(25)	Re(4)	9 249.4(10)	9 218.8(5)	502.6(10)
C(13A)	8 149(21)	2 444(13)	326(25)	O(50)	8 086(16)	9 698(9)	-554(18)
C(14A)	7 301(27)	2 855(15)	748(28)	O(60)	10 364(18)	9 283(10)	-142(22)
C(15A)	7 344(28)	3 622(16)	678(31)	O(70)	9 067(17)	8 365(9)	726(20)
C(16A)	8 191(30)	3 851(16)	254(31)	O(80)	9 426(16)	9 501(10)	1 997(18)
C(17A)	8 999(27)	3 478(16)	-181(28)	C(10B)	3 484(22)	1 717(12)	3 079(24)
C(18A)	8 962(25)	2 772(14)	-98(26)	C(20B)	2 510(30)	1 610(17)	2 182(33)
C(1B)	8 965(22)	7 519(13)	4 374(25)	C(30B)	3 600(31)	1 407(19)	4 550(36)
C(2B)	9 108(22)	7 353(12)	5 822(24)	O(10B)	4 161(17)	2 055(11)	2 759(20)

Cyclic voltammetry. The redox data for the compounds of Re and Os are given in Table 11. For $[\text{Re}(o\text{-pda})_3]^+$, two, reversible, one-electron reduction steps are observed, while for $\text{Re}(o\text{-pda})_3$ there is an oxidation and a reduction step (reversible, one-electron), with very similar respective potentials. This indicates that the chemically generated species evidently corresponds to the species produced by the electrochemical, one-electron reduction of the rhenium(vii) complex. The rhenium complexes also exhibit an irreversible oxidation at *c.a.* +0.45 V.

The cyclic voltammetry of $\text{Os}(\text{abt})_3$ agrees well with its formulation as an osmium(vi) species, since there are two reversible oxidations and two reversible reductions; we have been unable to isolate either oxidised or reduced species.

We have taken the redox processes to be metal related. Another alternative, equally simplistic, view is the consideration of these processes as purely ligand related. The theoretical potential limits of the electron-transfer series of $M[o\text{-}(\text{HN})_2\text{C}_6\text{H}_4]_2$ may be given by the reduced and oxidised forms of the ligands in combination with a stable valence state of the metal.² A more realistic approach may be to consider the electrochemical data in conjunction with molecular orbital models, as attempted by Stiefel *et al.*⁴ The redox processes would then involve the lowest unoccupied and highest occupied molecular orbitals. However, this approach has the limitation of the model used.

Experimental

Analyses by Pascher, Remagen, and Imperial College laboratories. Spectrometers: i.r., Perkin-Elmer 683, Perkin-Elmer 1720 (FT), spectra in Nujol mulls or KBr discs, in cm^{-1} , calibrated

against polystyrene; n.m.r., Bruker WM-250 (^1H , 250.13; ^{13}C , 62.90; ^{31}P , 101.3 MHz) and JEOL FX-900 (^1H , 89.55; ^{13}C , 22.51; ^{31}P , 36.21 MHz) (data in p.p.m. relative to SiMe_4 and 85% H_3PO_4 external); e.s.r., Varian E12 [X -Band, modulation amplitude 5 G (5×10^{-4} T), time constant 0.3 s]; electronic, Philips Scientific SP8-100 (10^{-5} mol dm^{-3}) solutions in MeCN, in 1-cm, matched quartz cells; bandwidth 2 nm). Conductivity: Data Scientific PT1-18 digital conductivity meter. Susceptibility measurements on solids were made at room temperature on an Evans balance; solution measurement for $\text{K}[\text{Re}(o\text{-pda})(o\text{-pbqd})_2]$ was made at room temperature by the Evans n.m.r. method. Cyclic voltammetry: in MeCN solutions on OE-PP2 instrument with 0.2 mol dm^{-3} $\text{NBu}_4^+\text{PF}_6^-$ in MeCN with platinum working, tungsten auxiliary, and silver pseudo-reference electrodes. Under these conditions, average E for ferrocene-ferrocenium = +0.46 V, with ΔE_v = 80 mV. This high value (theoretical value is 59 mV) is presumably due to uncompensated resistance in solution.²⁶ Melting points were determined in sealed tubes (under argon when necessary) and are uncorrected.

Reactions were normally carried out under oxygen-free nitrogen or argon; solvents were thoroughly degassed by nitrogen purge. Diethyl ether, thf, toluene, and hexane were dried by refluxing over sodium or sodium-benzophenone under nitrogen. Dichloromethane and acetonitrile were dried by refluxing over calcium hydride under nitrogen. Methanol was refluxed over magnesium. All solvents were distilled prior to use. Acetone was dried over molecular sieves (4A). The compounds Re_2O_7 ²⁷ and $\text{ReO}_3(\text{OSiMe}_3)_2$ ²⁸ were prepared by standard procedures.

Table 14. Fractional atomic co-ordinates ($\times 10^4$) for compound (2)

Atom	<i>x</i>	<i>y</i>	<i>z</i>
Re	181.6(3)	9 758.7(2)	9 148.0(2)
N(11)	86(7)	10 832(4)	9 672(3)
N(12)	-1 464(7)	10 323(4)	8 603(4)
N(21)	2 334(7)	9 921(4)	9 108(4)
N(22)	778(7)	9 391(4)	8 064(4)
N(31)	-1 089(8)	8 788(4)	9 182(4)
N(32)	447(7)	9 301(4)	10 247(4)
C(21)	3 081(8)	9 756(5)	8 440(4)
C(22)	2 178(9)	9 462(4)	7 836(5)
C(24)	4 227(11)	9 377(7)	6 970(6)
C(23)	2 752(10)	9 265(6)	7 090(5)
C(25)	5 097(11)	9 668(6)	7 550(7)
C(26)	4 562(9)	9 867(6)	8 306(6)
C(11)	-947(8)	11 379(5)	9 425(5)
C(12)	-1 819(9)	11 087(5)	8 820(5)
C(13)	-2 913(10)	11 581(6)	8 491(6)
C(14)	-3 094(11)	12 335(6)	8 761(6)
C(15)	-2 214(11)	12 623(6)	9 389(6)
C(16)	-1 134(11)	12 161(6)	9 706(6)
C(31)	-1 182(10)	8 347(5)	9 862(5)
C(32)	-322(9)	8 641(5)	10 469(5)
C(33)	-319(11)	8 259(6)	11 207(5)
C(34)	-1 168(12)	7 594(7)	11 319(6)
C(35)	-2 021(14)	7 295(6)	10 702(8)
C(36)	-2 057(12)	7 662(6)	9 999(7)
O(1)	4 344(8)	10 244(6)	465(4)
C(2)	4 640(17)	9 441(8)	717(9)
C(4)	5 652(11)	10 710(9)	525(7)
C(5)	6 789(14)	10 139(9)	858(12)
C(6)	6 027(16)	9 434(9)	1 137(9)
O(10)	3 480(8)	6 893(4)	2 549(5)
C(20)	4 452(14)	7 560(8)	2 474(8)
C(30)	3 552(14)	8 305(7)	2 657(7)
C(40)	2 438(14)	7 987(7)	3 228(9)
C(50)	2 212(14)	7 131(8)	2 992(8)

Tris(*o*-phenylenediamido)rhenium(VII) Perrhenate, (1).—(a) From $\text{ReO}_3(\text{OSiMe}_3)$. To a solution of $\text{ReO}_3(\text{OSiMe}_3)$ (1.2 g, 3.7 mmol) in thf (30 cm³) (with or without molecular sieves type 4A) was added, with stirring, *o*-C₆H₄(NH₂)₂ (1.2 g, 0.011 mol). The mixture turned deep green immediately, and after stirring for *ca.* 24 h was evaporated to dryness in air. The residue was washed with Et₂O (2 × 40 cm³) to remove unreacted ligand and extracted with acetone (Soxhlet). Most of the product is extracted within *ca.* 48 h, but extraction is not complete before *ca.* 80 h. Evaporation of the acetone solution from the extraction yields the product in sufficient purity for further reactions. Recrystallisation from acetone, thf, or methanol gives deep green/red dichroic prisms, which can be dried *in vacuo* or in air. Slow recrystallisation from acetone by evaporation of the solution in air is necessary to obtain *X*-ray quality crystals. Yield: 1.5 g, *ca.* 99% based on $\text{ReO}_3(\text{OSiMe}_3)$. I.r.: 3 296m (1 695m, acetone), 1 551s, 1 498w, 1 454m, 1 375m, 1 300s, 1 225m, 1 145s, 1 087(sh), 999w, 944w, 908s, 899s, 890s, 738m, 629s, 573s, 466m, and 370s cm⁻¹. Conductivity (10^{-3} mol dm⁻³ in MeCN, 23 °C): $\Lambda_M = 122 \text{ ohm}^{-1} \text{ cm}^2 \text{ mol}^{-1}$ (*cf.* NaBPh₄ under same conditions, $\Lambda_M = 102 \text{ ohm cm}^2 \text{ mol}^{-1}$).

(b) From Re_2O_7 . To a solution of Re_2O_7 (1.0 g, 2.09 mmol) in thf (10 cm³) containing molecular sieves was added an excess of *o*-C₆H₄(NH₂)₂ (1.47 g, 13.6 mmol) when the solution immediately became deep green. After stirring for *ca.* 12 h at room temperature, the solution was evaporated and the residue washed with Et₂O (4 × 20 cm³). Soxhlet extraction of the solid with acetone (*ca.* 100 cm³) followed by cooling (-20°C) gave the product. Yield 1.2 g, 77% based on Re_2O_7 .

(c) From NBuⁿ₄ReO₄. In thf with an excess of the diamine,

Table 15. Fractional atomic co-ordinates ($\times 10^4$) for compound (3)

Atom	<i>x</i>	<i>y</i>	<i>z</i>
Re	181.7(6)	-4 759.0(3)	-852.1(4)
N(11)	107(14)	-5 847(6)	-320(6)
N(12)	-1 473(12)	-5 321(8)	-1 397(7)
N(21)	2 336(12)	-4 940(6)	-871(8)
N(22)	754(14)	-4 387(8)	-1 943(8)
N(31)	-1 100(14)	-3 795(7)	-847(8)
N(32)	467(13)	-4 322(8)	256(7)
C(11)	-953(15)	-6 389(9)	-571(9)
C(12)	-1 812(16)	-6 085(10)	-1 197(9)
C(13)	-2 934(18)	-6 583(10)	-1 530(10)
C(14)	-3 108(19)	-7 348(11)	-1 226(11)
C(15)	-2 219(19)	-7 630(11)	-611(9)
C(16)	-1 125(19)	-7 181(10)	-287(10)
C(21)	3 052(15)	-4 771(11)	-1 557(9)
C(22)	2 151(15)	-4 467(9)	-2 179(9)
C(23)	2 760(19)	-4 272(11)	-2 927(9)
C(24)	4 226(19)	-4 370(11)	-3 056(11)
C(25)	5 150(21)	-4 685(13)	-2 446(11)
C(26)	4 601(19)	-4 881(10)	-1 701(9)
C(31)	-1 188(17)	-3 349(9)	-167(10)
C(32)	-316(18)	-3 662(9)	473(9)
C(33)	297(20)	-3 273(10)	1 227(10)
C(34)	-1 188(20)	-2 609(10)	1 331(12)
C(35)	-2 045(21)	-2 287(10)	725(13)
C(36)	-2 071(21)	-2 657(11)	-13(13)
O(1)	-674(14)	279(10)	-462(7)
C(1A)	-387(21)	-563(11)	-716(12)
C(2A)	1 051(27)	-558(17)	-1 124(17)
C(3A)	1 773(24)	180(16)	-865(18)
C(4A)	639(18)	757(18)	-528(14)
O(2)	-1 508(15)	-3 108(8)	-2 554(9)
C(1B)	-541(18)	-2 435(11)	-2 489(13)
C(2B)	-1 469(23)	-1 690(11)	-2 672(13)
C(3B)	-2 617(20)	-2 003(13)	-3 213(13)
C(4B)	-2 778(23)	-2 883(11)	-3 012(13)

prolonged reaction (*ca.* 7 d at room temperature) of the perrhenate gave the product in *ca.* 10% yield.

Reduction of [Re(o-pda)₃]⁺ to Re(o-pda)₃, (2).—To a solution of [Re(o-pda)₃][ReO₄] (1.5 g, 1.85 mmol) in thf (30 cm³) was added, while stirring, dispersed sodium metal (0.2 g, 8.7 mmol). After stirring for *ca.* 15 h, the violet mixture was filtered and evaporated in vacuum. The residue was extracted with thf (2 × 30 cm³) and the combined extracts filtered and the solvent removed under vacuum. The residue was extracted into CH₂Cl₂ (40 cm³), the extract filtered, concentrated until saturated, and cooled at -20 °C to yield a deep red-violet crystalline solid, which was collected, washed with hexane (2 × 10 cm³), and dried *in vacuo*. The mother-liquor provided further crops of the product. Yield 0.6 g, 65% based on [Re(o-pda)₃][ReO₄]. *X*-Ray quality crystals of the complex as its thf adduct were obtained from tetrahydrofuran layered with hexane. I.r.: 3 293m, 1 563m, 1 303m, 1 263s, 1 222w, 1 139s, 1 107m, 1 019m, 970w, 934w, 917w, 806m, 737s, 723s, 573(sh), and 456m cm⁻¹. Mass spectrum: *m/z* 505, [Re(HN)₂C₆H₄]₃⁺; 429, [Re(HN)₂C₆H₄]₂(NH)₂⁺; 108, C₆H₄(NH₂)₂⁺; 91, C₆H₄-(NH)⁺; and 80, C₅H₄(NH₂)⁺.

Oxidation of Re(o-pda)₃ to [Re(o-pda)₃]PF₆.—The salt AgPF₆ (0.1 g, 6.0×10^{-4} mol) was added to a stirred, red-violet solution of Re(o-pda)₃ (0.28 g, 5.55×10^{-4} mol) in thf (30 cm³). The mixture turns deep green immediately; the silver was recovered by filtration and the solvent removed. The residue was extracted with thf (30 cm³) and the extracts concentrated until saturated then cooled at -20 °C to give deep blue-

Table 16. Fractional atomic co-ordinates ($\times 10^4$) for compound (4)

Atom	<i>x</i>	<i>y</i>	<i>z</i>	Atom	<i>x</i>	<i>y</i>	<i>z</i>
Re(1A)	-0.4(11)	-3 070.3(7)	0.9(7)	C(15B)	1 102(27)	-2 985(27)	-6 767(17)
Re(1B)	1 575.6(10)	-2 861.0(6)	-4 373.0(7)	C(16B)	1 270(25)	-2 381(25)	-6 294(16)
N(11A)	1 100(18)	-3 569(16)	-29(13)	C(21B)	108(20)	-2 568(19)	-3 817(13)
N(12A)	145(19)	-3 533(18)	854(13)	C(22B)	280(20)	-3 527(18)	-3 669(13)
N(22A)	412(16)	-2 003(17)	-459(11)	C(23B)	-263(21)	-4 065(20)	-3 352(14)
N(21A)	-497(18)	-1 991(16)	344(11)	C(24B)	-1 025(25)	-3 689(24)	-3 194(16)
N(31A)	-187(19)	-3 659(19)	-794(12)	C(25B)	-1 186(26)	-2 743(26)	-3 354(17)
N(32A)	-1 015(16)	-3 750(14)	48(10)	C(26B)	-674(22)	-2 209(20)	-3 650(14)
N(11B)	1 465(18)	-2 217(15)	-5 162(13)	C(31B)	2 870(22)	-1 894(18)	-3 680(14)
N(12B)	1 640(17)	-3 888(16)	-4 984(11)	C(32B)	3 041(25)	-2 930(24)	-3 609(17)
N(21B)	665(18)	-2 149(16)	-4 138(11)	C(33B)	3 679(23)	-3 119(23)	-3 220(15)
N(22B)	981(17)	-3 727(15)	-3 908(11)	C(34B)	4 149(26)	-2 486(26)	-2 902(17)
N(31B)	2 216(17)	-1 793(16)	-4 075(11)	C(35B)	3 914(21)	-1 551(21)	-2 992(14)
N(32B)	2 502(15)	-3 414(14)	-3 987(11)	C(36B)	3 294(22)	-1 243(21)	-3 360(14)
C(11A)	1 430(19)	-3 799(17)	555(12)	K(1A)	-10(7)	-5 459(5)	93(4)
C(12A)	919(22)	-3 791(20)	1 023(14)	K(1B)	-1 907(6)	-2 103(5)	-405(4)
C(13A)	1 215(23)	-3 977(20)	1 609(14)	O(1)	-1 525(20)	-1 217(20)	-1 395(14)
C(14A)	1 974(24)	-4 213(23)	1 736(16)	C(11)	-1 626(31)	-225(33)	-1 402(22)
C(15A)	2 526(26)	-4 270(24)	1 249(19)	C(12)	-1 023(34)	109(34)	-1 952(23)
C(16A)	2 197(21)	-4 069(20)	663(15)	C(13)	-866(35)	-787(37)	-2 274(26)
C(21A)	-426(23)	-1 115(21)	103(15)	C(14)	-1 245(31)	-1 549(32)	-1 923(23)
C(22A)	143(24)	-1 091(21)	-329(17)	O(2)	-881(21)	-6 779(20)	-354(15)
C(23A)	409(24)	-277(23)	-634(16)	C(21)	-804(32)	-6 920(30)	-972(24)
C(24A)	41(20)	521(18)	-441(12)	C(22)	-1 474(35)	-7 498(37)	-1 256(24)
C(25A)	-502(22)	553(19)	12(14)	C(23)	-1 989(29)	-7 645(30)	-711(20)
C(26A)	-730(21)	-258(20)	325(14)	C(24)	-1 599(35)	-7 042(30)	-139(24)
C(31A)	-894(24)	-4 070(22)	-976(15)	O(3)	-3 941(26)	-2 157(27)	-6 634(19)
C(32A)	-1 321(21)	-4 134(19)	-449(14)	C(31)	-4 065(52)	-2 836(40)	-7 102(34)
C(33A)	-2 168(24)	-4 515(23)	-506(17)	C(32)	-3 353(41)	-2 734(40)	-7 473(27)
C(34A)	-2 417(26)	-4 879(24)	-1 126(17)	C(33)	-3 136(36)	-1 807(36)	-7 457(25)
C(35A)	-1 909(28)	-4 801(25)	-1 623(19)	C(34)	-3 561(33)	-1 498(32)	-6 971(24)
C(36A)	-1 153(24)	-4 415(23)	-1 540(16)	O(4)	1 482(24)	112(23)	6 043(16)
C(11B)	1 435(21)	-2 714(18)	-5 699(13)	C(41)	971(30)	146(29)	6 475(22)
C(12B)	1 451(21)	-3 687(20)	-5 617(14)	C(44)	1 722(28)	1 092(31)	5 961(20)
C(13B)	1 308(25)	-4 285(23)	-6 110(17)	C(43)	1 587(30)	1 511(28)	6 595(21)
C(14B)	1 155(23)	-3 907(23)	-6 695(14)	C(42)	991(32)	989(33)	6 834(22)

green/red dichromic prisms, which were collected, washed with Et_2O (10 cm^3), and dried *in vacuo*. Further crops were obtained from the mother-liquor. Yield 0.15 g, 83% based on $\text{Re}(o\text{-pda})_3$. I.r.: 3 333s, 1 553s, 1 500m, 1 456s, 1 374s, 1 300s, 1 226s, 1 145s, 999m, 937w, 841s, 774s, 726s, 626s, 572s, 557s, 459s, and 367s cm^{-1} . Conductivity ($10^{-3} \text{ mol dm}^{-3}$ in MeCN, 23 °C); $\Lambda_M = 135 \text{ ohm}^{-1} \text{ cm}^2 \text{ mol}^{-1}$.

Reaction of $[\text{Re}(o\text{-pda})_3][\text{ReO}_4]$ with Base.—(a) $\text{Re}(o\text{-pda})_2(o\text{-pbqd})$ (3). To a stirred solution of $[\text{Re}(o\text{-pda})_3][\text{ReO}_4]$ (0.5 g, 6.15×10^{-4} mol) in acetone (20 cm^3) was added a solution of KOH (0.09 g, 1.6 mmol) in MeOH (20 cm^3). The mixture turns deep red immediately. After stirring for *ca.* 24 h, the mixture was evaporated, the residue washed with Et_2O (40 cm^3) and extracted into toluene ($3 \times 50 \text{ cm}^3$). The combined red extracts were filtered, concentrated until saturated, and cooled at -20°C . The red precipitate was collected, washed with Et_2O (10 cm^3), and dried *in vacuo*. Recrystallisation from Me_2CO gives deep red prisms. Yield: 0.23 g, 74% based on $[\text{Re}(o\text{-pda})_3][\text{ReO}_4]$. I.r.: 3 264s (1 702s, Me_2CO), 1 594m, 1 561m, 1 512w, 1 481m, 1 466m, 1 438w, 1 384s, 1 300s, 1 262s, 1 213m, 1 182w, 1 150w, 1 125m, 1 102s, 1 020s, 938w, 911w, 878s, 863s, 806s, 740s, 700w, 655w, 602w, 583m, 568m, 519m, 468w, 453w, and 327w cm^{-1} . Mass spectrum: m/z 106, $\text{C}_6\text{H}_4(\text{NH})_2^+$; 105, $\text{C}_6\text{H}_4(\text{NH})\text{N}^+$; 91, $\text{C}_6\text{H}_4(\text{NH})^+$; 79, $\text{C}_5\text{H}_4(\text{NH})^+$; 27, HCN^+ ; 58, Me_2CO^+ ; and 43, MeCO^+ .

(b) $\text{K}[\text{Re}(o\text{-pda})(o\text{-pbqd})_2]$ (4). To a stirred solution of $\text{Re}(o\text{-pda})_2(o\text{-pbqd})$ (0.15 g, 2.98×10^{-4} mol) in acetone (20

cm^3) was added a solution of KOH (0.2 g, 3.57 mmol) in $\text{MeOH}-\text{thf}$ (1:1, 20 cm^3). After stirring for *ca.* 16 h, the red-brown mixture was evaporated to dryness. The residue was washed with Et_2O (40 cm^3) and extracted into CH_2Cl_2 (50 cm^3); the red-brown extract was filtered, concentrated until saturated, and cooled at -20°C . The red-brown, crystalline solid obtained was collected, washed with Et_2O (10 cm^3), and dried *in vacuo*. Yield 0.13 g, 81% based on $\text{Re}(o\text{-pda})_2(o\text{-pbqd})$. I.r.: 1 601m, 1 560m, 1 483s, 1 458m, 1 384s, 1 342w, 1 294s, 1 262s, 1 236w, 1 208w, 1 147w, 1 124m, 1 104s, 1 020s, 904w, 849s, 806s, 752s, 735s, 691m, 669m, 649m, 626w, 585m, 561s, 544m, 523s, 463m, 451w, and 408w cm^{-1} . Conductivity ($10^{-3} \text{ mol dm}^{-3}$ in MeCN, 24 °C): $\Lambda_M = 100 \text{ ohm}^{-1} \text{ cm}^2 \text{ mol}^{-1}$.

[Re(abt)₃] (5).—To a stirred solution of $\text{ReO}_3(\text{OSiMe}_3)$ (0.9 g, 2.78 mmol) in thf (35 cm^3) with molecular sieves (4A, *ca.* 2 g) was added *o*-aminobenzenethiol (1.2 cm^3 , 0.011 mol). The mixture turned deep green immediately, and after *ca.* 24 h was evaporated, the residue washed with hexane (30 cm^3) and extracted into toluene ($2 \times 40 \text{ cm}^3$). The deep blue-green extracts were combined, filtered, concentrated until saturated, and cooled at -20°C . The crystalline solid was collected, washed with hexane (*ca.* 10 cm^3), and dried *in vacuo*. Recrystallisation from Et_2O containing *ca.* 5% thf gave deep blue/purple dichroic prisms; X-ray quality crystals were best obtained in recrystallisations by slow evaporation of acetone solutions in air. Yield: 1.33 g, 86% based on $\text{ReO}_3(\text{OSiMe}_3)$. I.r.: 3 225m, 1 547m, 1 352s, 1 308w, 1 267s, 1 230m, 1 159m, 1 128s,

Table 17. Fractional atomic co-ordinates ($\times 10^4$) for compound (5)

Atom	<i>x</i>	<i>y</i>	<i>z</i>
Re	-9 040.8(8)	-7 867.8(8)	-7 619.7(5)
S(1)	-6 951(5)	-8 003(6)	-8 054(3)
S(2)	-9 371(6)	-9 438(5)	-8 606(3)
S(3)	-8 487(6)	-9 329(5)	-6 604(4)
N(1)	-8 555(14)	-6 163(13)	-7 622(11)
N(2)	-10 523(14)	-7 325(15)	-8 308(8)
N(3)	-10 078(18)	-7 411(17)	-6 577(10)
C(11)	-6 480(22)	-6 553(20)	-8 051(13)
C(12)	-5 257(20)	-6 165(26)	-8 312(12)
C(13)	-5 047(25)	-4 953(25)	-8 302(17)
C(14)	-6 041(31)	-4 155(22)	-8 068(14)
C(15)	-7 161(22)	-4 517(20)	-7 840(13)
C(16)	-7 420(20)	-5 727(20)	-7 837(13)
C(21)	-10 789(22)	-9 031(19)	-9 106(13)
C(22)	-11 460(23)	-9 790(25)	-9 652(13)
C(23)	-12 557(21)	-9 381(23)	-9 970(13)
C(24)	-12 962(24)	-8 201(20)	-9 804(14)
C(25)	-12 343(19)	-7 510(18)	-9 272(12)
C(26)	-11 212(17)	-7 900(24)	-8 886(11)
C(31)	-9 316(26)	-8 943(19)	-5 697(12)
C(32)	-9 226(29)	-9 479(18)	-4 885(15)
C(33)	-9 966(30)	-9 053(25)	-4 174(15)
C(34)	-10 723(28)	-8 160(21)	-4 315(17)
C(35)	-10 865(23)	-7 537(18)	-5 095(11)
C(36)	-10 084(17)	-7 920(22)	-5 772(11)

1 064s, 968w, 915w, 885w, 861w, 843w, 805w, 765s, 751s, 724s, 648w, 571s, 536w, 453m, 440w, and 323m cm^{-1} .

Os(abt)₃ (6).—To a stirred solution of OsO_4 (1.02 g, 4.0 mmol) in thf (35 cm³) with molecular sieves (4A, *ca.* 2 g) was added *o*-aminobenzenethiol (2.6 cm³, 0.024 mol). The mixture, which turned deep red immediately, was evaporated after *ca.* 20 h; the residue was washed with hexane (30 cm³) and extracted with CH_2Cl_2 (2 × 40 cm³). The deep red extracts were filtered, concentrated until saturated, and cooled at -20 °C to give clusters of spear-shaped red crystals of the CH_2Cl_2 adduct which were collected, washed with hexane (20 cm³), and dried *in vacuo*. Yield 2.32 g, 90% based on OsO_4 . I.r.: 3 231m, 1 543m, 1 431m, 1 384m, 1 341m, 1 317m, 1 259s, 1 244s, 1 217s, 1 153m, 1 119s, 1 061s, 1 020(sh), 925w, 860w, 843w, 801w, 750vs, 718s, 685s, 656s, 577s, 565s, 531m, 453s, 432s, and 386s cm^{-1} . Mass spectrum: *m/z* 124, $\text{C}_6\text{H}_4(\text{SH})(\text{NH})^+$; 84, CH_2Cl_2^+ ; and 49, CH_2Cl^+ .

trans-Dioxo(*o*-phenylenediamido)osmium(viii) (7).—To a stirred solution of OsO_4 (0.78 g, 3.1 mmol) with molecular sieves was added *o*- $\text{C}_6\text{H}_4(\text{NH}_2)_2$ (1.38 g, 0.013 mol). The mixture turned deep purple immediately, and then deep reddish brown. After *ca.* 20 h it was evaporated, the brown residue washed with Et_2O (40 cm³), then Soxhlet extracted with acetone which was then removed. Yield 0.94 g, 71% based on OsO_4 . I.r.: 3 312s, 3 298s, 3 277s, 1 584m, 1 476s, 1 385w, 1 347w, 1 284s, 1 160w, 1 110m, 1 018m, 922m, 865vs, 805s, 759s, 742s, 707s, 673s, 648s, 574s, 461s, and 340m cm^{-1} .

X-Ray Crystallography.—All X-ray measurements were made using a CAD4 diffractometer operating in the ω –2θ scan mode, with Mo-K α radiation, on crystals sealed under argon in thin-walled glass capillaries. Following preliminary photography, orientation matrices and associated cell dimensions and intensity data were obtained following previously detailed procedures.²⁹ Empirical absorption corrections were applied. The structures were determined *via* application of the heavy-atom method and refined using least-squares procedures. For

Table 18. Fractional atomic co-ordinates ($\times 10^4$) for compound (6)

Atom	<i>x</i>	<i>y</i>	<i>z</i>
Os	-266.6(4)	-1 206.7(6)	0.0
S(1)	-225(4)	-1 485(6)	1 543(4)
S(2)	-460(3)	1 186(4)	-103(6)
S(3)	-411(3)	-3 568(5)	-209(3)
N(1)	1 040(9)	-971(13)	233(8)
N(2)	-1 560(9)	-1 088(15)	90(27)
C(1)	874(11)	-1 322(19)	1 752(11)
C(2)	1 443(12)	-1 054(17)	983(12)
C(3)	2 352(14)	-916(23)	1 131(12)
C(4)	2 655(23)	-1 109(25)	1 934(17)
C(5)	2 171(18)	-1 323(24)	2 670(14)
C(6)	1 257(14)	-1 489(17)	2 567(12)
C(7)	-1 613(10)	1 303(15)	-27(31)
C(8)	-2 050(11)	61(14)	41(32)
C(9)	-3 010(13)	34(19)	136(25)
C(10)	-3 431(11)	1 315(20)	6(36)
C(11)	-2 961(14)	2 509(22)	29(30)
C(12)	-2 066(15)	2 543(20)	-54(34)
C(13)	-200(11)	-3 641(19)	-1 317(14)
C(14)	53(12)	-2 440(21)	-1 743(15)
C(15)	244(17)	-2 473(23)	-2 657(15)
C(16)	198(14)	-3 612(35)	-3 121(18)
C(17)	-30(22)	-4 852(32)	-2 679(21)
C(18)	-217(17)	-4 908(26)	-1 791(20)
N(3)	-46(18)	-1 237(25)	-1 251(21)
C(19)	-2 509(28)	-3 679(31)	-1 886(28)
C(20)	-2 226(28)	-2 329(34)	-2 319(28)
C(21)	-2 622(24)	-4 943(41)	-2 515(23)
O(2)	2 646(28)	-3 693(26)	-1 055(25)

[$\text{[Re(o-pda)}_3\text{][ReO}_4\cdot\text{Me}_2\text{CO}$, in which the structure contains two formula units per asymmetric unit, the refinement was blocked with parameters for one $[\text{Re}(o\text{-pda})_3]^+$ cation in each of two blocks and parameters for the two ReO_4 and acetone units in a third. All atoms were refined anisotropically and no hydrogens were included. The rather poor diffracting power of the crystals resulted in a smaller portion of data being observed than would be preferred and thus a low parameter to variable ratio. For $\text{Re}(o\text{-pda})_3$, Re(abt)_3 , and Os(abt)_3 full-matrix refinement was used with all atoms refined anisotropically. Hydrogens were included in idealised positions only in the case of $\text{Re}(o\text{-pda})_3$. In the case of Os(abt)_3 , the refinement was troublesome due to the pseudo-symmetric arrangement of the molecule in the $Pna2_1$ unit cell (one complete ligand lay in a plane, with the Os atom, perpendicular to *c*). Details of the crystal data, data collection, and refinement are given in Table 12. Fractional atomic co-ordinates are given in Tables 13–18.

Additional material available from the Cambridge Crystallographic Data Centre comprises H-atom co-ordinates and thermal parameters.

Acknowledgements

We thank Johnson Matthey plc for the loan of osmium, and the S.E.R.C. for support and provision of *X*-ray facilities.

References

- J. A. McCleverty, *Prog. Inorg. Chem.*, 1968, **10**, 49; R. H. Holm and M. J. O'Connor, *ibid.*, 1971, **14**, 241. See also 'Comprehensive Coordination Chemistry,' eds. G. Wilkinson, R. D. Gillard, and J. A. McCleverty, Pergamon, Oxford, 1987, vol. 2; F. A. Cotton and G. Wilkinson, 'Advanced Inorganic Chemistry,' 5th edn., Wiley, New York, 1988.
- A. L. Balch and R. H. Holm, *J. Am. Chem. Soc.*, 1966, **88**, 5201; G. S. Hale and R. H. Soderberg, *Inorg. Chem.*, 1968, **7**, 2300.

- 3 (a) J. K. Gardner, N. Pariyadath, J. L. Corbin, and E. I. Stiefel, *Inorg. Chem.*, 1978, **17**, 897; (b) J. Baldas, J. F. Boas, J. Bonnyman, J. R. Pilbrow, and G. A. Williams, *J. Am. Chem. Soc.*, 1985, **107**, 1886.
- 4 E. I. Stiefel, R. Eisenberg, R. C. Rosenberg, and H. B. Gray, *J. Am. Chem. Soc.*, 1966, **88**, 2956.
- 5 G. G. Christoph and V. L. Goedken, *J. Am. Chem. Soc.*, 1973, **95**, 3869.
- 6 M. Zehnder and H. Loliger, *Helv. Chim. Acta*, 1980, **63**, 754.
- 7 (a) R. Eisenberg and J. A. Ibers, *Inorg. Chem.*, 1966, **5**, 411; (b) E. I. Stiefel and H. B. Gray, *J. Am. Chem. Soc.*, 1965, **87**, 4012.
- 8 L. A. de Learie, R. C. Haltiwanger, and C. G. Pierpont, *Inorg. Chem.*, 1987, **26**, 817.
- 9 (a) A. J. Nielson and W. P. Griffith, *J. Chem. Soc., Dalton Trans.*, 1978, 1501; (b) M. B. Hursthouse, T. Fran, L. New, W. P. Griffith, and A. J. Nielson, *Transition Met. Chem. (Weinheim, Ger.)*, 1978, **3**, 253.
- 10 E. J. Rosa and G. N. Schrauzer, *J. Phys. Chem.*, 1969, **73**, 3132.
- 11 B. J. McCaffrick and D. S. Rinehart, *J. Inorg. Nucl. Chem.*, 1980, **42**, 928.
- 12 B. N. Figgis and J. Lewis, *Prog. Inorg. Chem.*, 1964, **6**, 139.
- 13 G. Rouschias, *Chem. Rev.*, 1974, **74**, 531.
- 14 S. E. Livingstone and J. D. Nolan, *Aust. J. Chem.*, 1973, **26**, 961.
- 15 G. N. Lamar and W. D. Horrocks, 'NMR of Paramagnetic Molecules: Principles and Applications,' Academic Press, New York, 1973, ch. 4.
- 16 K. Yamanouchi and J. H. Enemark, *Inorg. Chem.*, 1978, **17**, 2911.
- 17 E. I. Stiefel and G. F. Brown, *Inorg. Chem.*, 1972, **11**, 434.
- 18 R. Hoffman, J. M. Howell, and A. R. Rossi, *J. Am. Chem. Soc.*, 1976, **98**, 2484.
- 19 M. Cowie and M. J. Bennett, *Inorg. Chem.*, 1976, **15**, (a) 1584; (b) 1584; (c) 1595.
- 20 J. Baldas, J. Boas, J. Bonnyman, M. F. Mackay, and G. A. Williams, *Aust. J. Chem.*, 1982, **35**, 2413; J. H. Welch, R. D. Bereman, and P. Singh, *Inorg. Chem.*, 1988, **27**, 2862.
- 21 K. W. Chiu, W. K. Wong, G. Wilkinson, A. M. R. Galas, and M. B. Hursthouse, *Polyhedron*, 1982, **1**, 37.
- 22 R. Eisenberg and H. B. Gray, *Inorg. Chem.*, 1967, **6**, 1844.
- 23 R. J. Collins, J. Jones, and W. P. Griffith, *J. Chem. Soc., Dalton Trans.*, 1974, 1094; W. P. Griffith and R. Rossetti, *ibid.*, 1972, 1449; W. P. Griffith, *J. Chem. Soc. A*, 1969, 211.
- 24 G. F. Brown and E. I. Stiefel, *Inorg. Chem.*, 1973, **12**, 2140.
- 25 J. F. Gibson, G. M. Lack, K. Mertis, and G. Wilkinson, *J. Chem. Soc., Dalton Trans.*, 1976, 1492; P. Stavropoulos, P. G. Edwards, T. Behling, G. Wilkinson, M. Mottevalli, and M. B. Hursthouse, *ibid.*, 1987, 169.
- 26 A. J. Bard and L. R. Faulkner, 'Electrochemical Methods,' Wiley, New York, 1980.
- 27 A. D. Melaven, J. N. Fowle, W. Bricknell, and C. F. Hiskey, *Inorg. Synth.*, 1950, **3**, 188.
- 28 H. Schmidt and H. Schmidbauer, *Chem. Ber.*, 1959, **92**, 2667.
- 29 M. B. Hursthouse, R. A. Jones, K. M. A. Malik, and G. Wilkinson, *J. Am. Chem. Soc.*, 1979, **101**, 4128.

Received 21st March 1989; Paper 9/01203F